Rates and timing of chlorophyll-*a* increases~~growth rates~~ and related environmental variables in global temperate and cold-temperate lakes

Hannah Adams[1], Jane Ye[1], Bhaleka Persaud[1], Stephanie Slowinski[1], Homa Kheyrollah Pour[2], Philippe Van Cappellen[1]

[1] Ecohydrology Research Group, Department of Earth and Environmental Sciences and Water Institute, University of Waterloo, Waterloo, ON, Canada

[2] ReSEC Research Group, Department of Geography and Environmental Studies, Wilfrid Laurier University, Waterloo, ON, Canada

Correspondence to: Hannah Adams (hadams21@mun.ca)

Running Head: Chlorophyll-*a* concentrations~~growth rates~~ in northern~~mid-to-high latitude~~ lakes

Keywords: northern lakes,~~lake~~ primary productivity, chlorophyll-*a* concentration, increase~~,~~ ~~growth window, growth~~ rate, ~~bottom-up controls,~~ trophic state, climate change~~ice phenology, solar irradiance~~

Abstract

Lakes are key ecosystems within the global biogeosphere. However, the environmental~~bottom-up~~ controls on the biological productivity of lakes, including surface temperature, ice phenology, nutrient loads and mixing regime, are increasingly altered by climate warming and land-use changes. To better characterize global trends in~~understand the environmental drivers of~~ lake productivity, we assembled a dataset on chlorophyll-*a* concentrations, as well as associated water quality parameters and surface solar radiation~~irradiance~~, for temperate and cold-temperate lakes experiencing seasonal ice cover. We developed a method to identify periods of rapid net increase of ~~algal growth from~~ *in situ* chlorophyll-*a* concentrations from time series data and applied it to data collected~~measurements performed~~ between 1964 and 2019 across 343~~357~~ lakes~~, predominantly~~ located north of 40°. The data ~~Long-term trends~~ show that the spring chlorophyll-*a* increase periods~~algal growth windows~~ have been occurring earlier in the year, ~~thus~~ potentially extending the growing season and increasing the annual productivity of northern lakes. The dataset on~~is also used to analyze the relationship between chlorophyll-a growth rates and solar irradiance. Lakes of higher trophic status exhibit a higher sensitivity to solar radiation, especially at moderate irradiance values during spring. The lower sensitivity of~~ chlorophyll-*a* increase rates and timing ~~growth rates to solar irradiance in oligotrophic lakes likely reflects the dominant role of nutrient limitation. Chlorophyll-a growth rates are significantly influenced by light availability in spring but not in summer and fall, consistent with a switch to top-down control of summer and fall algal communities. The growth window dataset~~ can be used to analyze trends and patterns in lake productivity across the northern hemisphere or at smaller, regional scales. We illustrate~~present~~ some ~~general~~ trends extracted from~~in~~ the dataset~~data~~ and encourage other researchers to use the open dataset for their own research questions.

1 Introduction

Lakes play an important role in the biogeochemical cycling of many elements (Battin et al., 2008; Cole et al., 2007; O'Connell et al., 2020; Rousseaux and Gregg, 2013; Schindler, 1971). With over 100 million documented lakes on earth (Verpoorter et al., 2014), evidence indicates that the majority of global lakes are shallow with enough light and nutrients available to make them highly productive ecosystems (Downing et al., 2006; Wetzel, 2001). Lakes therefore represent active sites for the storage, transport, and transformation of carbon, nutrients (e.g., nitrogen, phosphorus, silicon, iron), and contaminants (e.g., mercury) along the freshwater continuum (Lauerwald et al., 2019; Tranvik et al., 2009). They are also sensitive to the effects of climate change (Williamson et al., 2009; Rouse et al., 1997).~~Lakes play an important role in the biogeochemical cycling of many elements (Battin et al., 2008; Cole et al., 2007; O'Connell et al., 2020; Rousseaux and Gregg, 2013; Schindler, 1971). With over 100 million documented lakes on earth (Verpoorter et al., 2014), evidence indicates that the majority of global lakes are shallow with enough light and nutrients available to make them highly productive ecosystems (Downing et al., 2006; Wetzel, 2001). Lakes therefore represent active sites for the storage, transport, and transformation of carbon, nutrients (e.g., nitrogen, phosphorus, silicon, iron), and contaminants (e.g., mercury) along the freshwater continuum (Lauerwald et al., 2019; Tranvik et al., 2009).~~

There are multiple environmental controls on lake primary productivity, including water temperature, ice phenology, nutrient concentrations, circulation, mixing regime, and solar radiation (Lewis, 2011; Zohary et al., 2009). Stressors such as climate change and nutrient pollution can significantly impact these controls, altering the ecosystem structure and biogeochemical functioning of lakes (Jeppesen et al., 2020; Markelov et al., 2019). Changes affecting northern lakes include warmer water temperatures, enhanced stratification and hypoxia, nutrient enrichment, light attenuation by chromophoric organic matter, and increases in the relative abundance of toxic cyanobacteria in the phytoplankton community (Deng et al., 2018; Huisman and Hulot, 2005; Jeppesen et al., 2003; Creed et al., 2018). For example, Lake Superior has seen an increase in primary production during the last century, together with increasing surface water temperatures and longer seasonal stratification and ice-free periods (O'Beirne et al., 2017). Other lakes are similarly experiencing increases in productivity. According to Lewis (2011), the current mean primary production of lakes is 260 g C m^{-2} y^{-1}, which is 162% higher than earlier estimations under historical baseline conditions.~~There are multiple bottom-up~~

~~controls on lake primary productivity, including water temperature, ice phenology, nutrient concentrations, circulation, mixing regime, and solar radiation (Lewis, 2011). Stressors such as climate change and nutrient pollution can significantly impact these controls, altering the ecosystem structure and biogeochemical functioning of lakes (Jeppesen et al., 2020; Markelov et al., 2019). Changes affecting northern lakes include warmer water temperatures, enhanced stratification and hypoxia, nutrient enrichment, light attenuation by chromophoric organic matter, and increases in the relative abundance of toxic cyanobacteria in the phytoplankton community (Deng et al., 2018; Huisman and Hulot, 2005; Jeppesen et al., 2003; Creed et al., 2018). For example, Lake Superior has seen an increase in primary production during the last century, together with increasing surface water temperatures and longer seasonal stratification and ice-free periods (O'Beirne et al., 2017). Other lakes are similarly experiencing increases in productivity. According to Lewis (2011), the current mean primary production of lakes is 260 g C m~~$^{-2}$~~y~~$^{-1}$~~, which is 162% higher than earlier estimations under historical baseline conditions.~~

Globally, phytoplankton (i.e., algae) are the main primary producers in lakes and generally make up the foundation of lentic food webs (Carpenter et al., 2016). Periods of high lake productivity coincide with a rapid increase in phytoplankton biomass. In extreme cases, algal blooms can reach hundreds to thousands of cells per milliliter (Henderson-Seller and Markland, 1987). These bloom events produce large quantities of decomposing organic matter that cause the expansion of hypoxic conditions within the lake (Watson et al., 2016). In harmful algal blooms, certain algal species also release hepatotoxic and neurotoxic compounds (Codd et al., 2005). Thus, identifying trends in the timing and intensity of seasonal algal growth, and linking them to changes in environmental stressors, can help predict the future of lake productivity and assess the risk of undesirable algal blooms.~~Phytoplankton (i.e., algae) are the main primary producers in lakes and generally make up the foundation of lentic food webs (Carpenter et al., 2016). Periods of high lake productivity coincide with a rapid increase in phytoplankton biomass. In extreme cases, algal blooms can reach hundreds to thousands of cells per milliliter (Henderson-Seller and Markland, 1987). These bloom events produce large quantities of decomposing organic matter that cause the expansion of hypoxic conditions within the lake (Watson et al., 2016). In harmful algal blooms, certain algal species also release hepatotoxic and neurotoxic compounds (Codd et al., 2005). Thus, identifying trends in the timing and intensity of seasonal algal growth, and~~

~~linking them to changes in environmental stressors, can help predict the future of lake productivity and assess the risk of undesirable algal blooms.~~

Because it is challenging to measure algal abundance and growth directly, chlorophyll-*a* is often used as a proxy for algae biomass and an indicator of the associated primary production in lakes (Huot et al., 2007). Although other proxies have been developed (Lyngsgaard et al., 2017), chlorophyll-*a* is the most common metric to characterize trends in algal biomass within and across lakes, especially in historical water quality records. Tett (1987) proposes a chlorophyll-*a* threshold of 100 µg L^{-1} to define “exceptional blooms”, Jonsson et al. (2009) use a threshold of 5 µg L^{-1} to identify a bloom, while Binding et al. (2021) flags an algal bloom when the chlorophyll-*a* concentrations extracted from satellite observations exceed 10 µg L^{-1}. Such threshold values, however, do not take into account the baseline (i.e., no-bloom) chlorophyll-*a* concentration specific to a given lake, or the lake’s trophic status (Germán et al., 2017). Furthermore, focusing on harmful and nuisance algal blooms alone may mask the impact that a changing climate or other stressors may have on a lake’s overall biological productivity.~~Because it is challenging to measure algal population growth directly, chlorophyll-*a* is often used as a proxy for both the algae biomass and the associated primary production rate in lakes (Huot et al., 2007). Although other proxies have been developed (Lyngsgaard et al., 2017), chlorophyll-*a* is the most common metric to characterize trends in algal biomass within and across lakes, especially in historical water quality records. Tett (1987) proposes a chlorophyll-*a* threshold of 100 µgL^{-1} to define “exceptional” blooms”, Jonsson et al. (2009) use a threshold of 5 µgL^{-1} to identify a bloom, while Binding et al. (2021) flags an algal bloom when the chlorophyll-*a* concentrations extracted from satellite observations exceed 10 µgL^{-1}. Such threshold values, however, do not take into account the baseline (i.e., no-bloom) chlorophyll-*a* concentration specific to a given lake, or the lake’s trophic status (German et al., 2017). Furthermore, focusing on harmful and nuisance algal blooms alone may mask the impact that a changing climate or other stressors may have on a lake’s overall biological productivity.~~

Intra-annual fluctuations in lake chlorophyll-*a* concentration result from the interactions of multiple variables and processes including grazing by zooplankton, competition between algal species with different growth strategies and chlorophyll-*a* contents, and changes in temperature, light, and nutrient availability (Lyngsgaard et al., 2017; Sommer et al., 1986). In dimictic lakes, for example, there are usually two peaks in algal biomass, and hence also in chlorophyll-*a* concentrations, in the spring and fall, with a smaller biomass stock of slower growing species during the summer, and an even smaller stock of algae (in terms of both biovolume and chlorophyll-*a*) under the ice cover in the winter (Hampton et al., 2017).

The spring increase in algal biomass generally consists of fast-growing algal species that take advantage of the increases in temperature and light following ice-off, as well as the available inorganic nutrients that were generated by mineralization under the ice over the winter. The shift from spring to summer algal communities often coincides with high zooplankton grazing rates exceeding the spring algal growth rates, hence, bringing down the total algal biomass. The high zooplankton grazing rates favor the growth during the summer of algal species that are less edible by grazers, but which tend to grow at slower rates. Lake overturn in the fall initiates the transition from the predominance of the slow growing species in the summer to the fast-growing phytoplankton species in the fall causing a second peak in algal biomass (Sommer et al., 1986). ~~Annual fluctuations in lake chlorophyll-*a* concentration are an indicator of the natural seasonal succession of algal species as a function of temperature, light, and nutrient availability (Lyngsgaard et al., 2017). For instance, in a dimictic lake algal growth in the spring tends to be controlled by these bottom-up controls, with light often being the primary limiting factor, while later in the summer or fall algal biomass may be more influenced by zooplankton grazing (i.e., a top-down control), while nutrient availability may overtake solar radiation as the limiting resource for growth (Lewis et al., 2018; Lyngsgaard et al., 2017; Scofield et al., 2020).~~

A common approach for comparing chlorophyll-*a* trends across multiple lakes is to consider the maximum or mean annual chlorophyll-*a* concentrations. For example, Ho et al. (2019) applied~~(2020) used~~ the Mann-Kendall trend test to analyze time series of annual maximum chlorophyll-*a* concentrations, while Shuvo et al. (2021) used a random forest regression approach to assess the relative importance of climatic versus non-climatic controls on mean chlorophyll-*a* concentrations. Both these studies analyzed chlorophyll concentrations derived from satellite observations rather than measured *in situ*. In addition~~However~~, these approaches did~~do~~ not specifically identify~~look at~~ the periods of the year when chlorophyll-*a* concentrations experienced~~algal biomass is primarily determined by bottom-up controls and exhibits~~ rapid changes~~growth~~.

Alternatively, the rate of increase~~change~~ in chlorophyll-*a* concentration can be used to constrain~~capture~~ the timing of rapid increase in algal biomass usually associated with periods of high primary~~lake~~ productivity. In this study, we refer to these as “periods of chlorophyll-*a* increase” (PCIs).~~as “growth windows”.~~ The weeks leading up to a PCI~~growth window~~ are crucial to create the necessary ~~environmental~~ conditions that enable algal growth (Lewis et al., 2018).~~(Lewis et al., 2018).~~ Thus, to analyze trends in lake net primary productivity, one should consider environmental variables, such as surface water temperature, solar radiation, and nutrient concentrations, both during and preceding the annual PCIs~~growth windows~~.

Although the rate of chlorophyll-*a* concentration increase~~growth~~ has been used to detect algal blooms within individual water bodies, for example in the San Roque reservoir (Germán et al., 2017), it has rarely been used across large temporal (i.e., more than a few years) and spatial (i.e., regional and up) scales. Here, we present a method for calculating net rates of~~seasonal~~ chlorophyll-*a* increase (RCI). The timing of PCIs ~~growth rates~~ and values of the corresponding RCIs were~~then create a dataset of these rates~~ derived from *in situ* chlorophyll-*a* concentrations obtained for 343~~in 357~~ lakes located~~, most of which are~~ at latitudes above 40° N. The entire dataset covers the period from 1964 to 2019, and further contains data on coincident ~~bottom-up~~ environmental control variables, including ~~*in situ*~~ surface solar radiation.~~ measurements.~~ To illustrate the potential applications of the resulting dataset, we present some temporal~~general~~ trends of the chlorophyll-*a* rates and their relationships with environmental variables. The dataset is made available as an open resource that other researchers are encouraged to use in their own work.

2 Data and methods

All data processing, visualizations, and analyses were carried out with Python (ver. 3.7.6; Python Software Foundation, 2021) using the pandas library (Reback et al., 2020), NumPy library (Harris et al., 2020), and Dplython library (Riederer, 2015), while QGIS/PYQGIS was used for all spatial data analyses (ver. 3.16; QGIS Development Team, 2021).~~All data processing, visualizations, and analyses were carried out with Python (ver. 3.7.6; Python Software Foundation, 2021) using the pandas library (Reback et al., 2020), NumPy library (Harris et al., 2020), and Dplython library (Riederer, 2015), while QGIS/PYQGIS was used for all spatial data analyses (ver. 3.16; QGIS Development Team, 2021).~~

2.1 Data acquisition, compilation, and quality control

2.1.1 Lake data selection

In situ chlorophyll-*a* concentrations and other lake physico-chemical data were extracted from open source international, national, and regional databases (see supplementary information for a summary of all databases used). The data include surface water temperature, Secchi depth and pH, as well as the concentrations of particulate organic carbon (POC), total phosphorus (TP), soluble reactive phosphorus (SRP), total Kjeldahl nitrogen (TKN) and dissolved organic carbon (DOC).

To enable readers to compare the methods used by different lake monitoring agencies and researchers to collect and process *in situ* samples, we provide the links to the raw data sources and metadata files in the supplementary information. When selecting data, we tried to be as consistent as possible by implementing the following steps (more details can be found in the "initial formatting" folder found in the associated GitHub repository).

1) We only included measurements taken at ≤ 3 m water depth. When the sampling depth was not provided, we assumed the sample was taken from within the top 0.5-3 m of the lake, given that this is the usual standard sampling protocol (Dorset Environmental Science Centre, 2010; United States Environmental Protection Agency, 2012).
2) We selected lakes from mid-to-high latitudes (≥ 40° N). Lakes at these latitudes typically experience seasonal ice cover and thermal stratification during the summer, in contrast to low-latitude lakes that are typically meromictic or polymictic (Woolway and Merchant, 2019).

~~*In situ* chlorophyll-*a* concentrations and other lake physico-chemical data were collected from open source international, national, and regional databases. The data include surface water temperature, Secchi depth and pH, as well as the concentrations of particulate organic carbon (POC), total phosphorus (TP), soluble reactive phosphorus (SRP), total Kjeldahl nitrogen (TKN) and dissolved organic carbon (DOC). We selected lakes from latitudes ≥ 40° N to reduce the latitude-dependent variability in mixing and thermal regimes, both of which exert a strong control on lake productivity (Kirillin et al., 2012). At mid-to-high latitudes most lakes are dimictic with seasonal ice cover while low-latitude lakes are typically meromictic or polymictic (Woolway and Merchant, 2019). High-elevation lakes at lower latitudes can experience similar~~

~~effects from the transition from winter to spring, even without ice cover (Deng et al., 2020). We therefore included the extensively monitored Lake Kasumigaura in Japan and Lake Taihu in China in our study, although they are located at latitudes lower than 40°N.~~

~~Chlorophyll-*a* measurements are collected at variable water depths by different lake monitoring agencies and researchers. For consistency, we only included measurements taken at ≤ 3 m depth. When the sampling depth was not provided, we assumed the sample was taken from within the top 0.5-3 m of the lake, given that this is standard sampling protocol (Dorset Environmental Science Centre, 2010; United States Environmental Protection Agency, 2012).~~

We omitted all variable values below the corresponding analytical detection limit. Data from different sources were individually reformatted to yield consistent (standard) units and headings. Where needed, reported values were averaged to yield daily mean values ~~mean~~ before being combined into a single csv file. When multiple chlorophyll-*a* data types were available (as, for example, in the Laurentian Great Lakes data series), we selected the uncorrected data because most reported lake chlorophyll-*a* concentrations have not been corrected for phaeophytin pigments. If no coordinates were provided, we assigned those of the lake centroid in QGIS.~~ or estimated based on the location name.~~ Fifteen lakes had unknown~~no known~~ location and were removed from the final dataset. We further restricted ourselves to lakes that in most years were sampled at least 6~~8~~ times per year, which~~. This~~ was considered~~found to be~~ the minimum ~~number of~~ sampling frequency~~points required~~ to reliably detect the yearly PCIs~~growth windows. The location of all lake sampling locations in the growth window dataset are shown in Figure 1~~.

With~~After~~ the above selection criteria~~and quality assessments~~, the final dataset ~~used for calculating the growth windows~~ contained 52116 potential PCIs~~unique data points (62% of the original data)~~ for 343~~357~~ lakes at~~, all~~ ≥ 40°N ~~(except Lake Kasumigaura~~ and ~~Lake Taihu),~~ covering the period 1964-2019. The location of the lake sampling locations in the PCI dataset are shown in Figure 1.

2.1.2 Surface solar radiation data

Open source *in situ* surface solar radiation (SSR) data for the period 1950-2020 were collected from stations paired with the selected lakes. Each lake was paired with the closest SSR station using the nearest neighbor function in QGIS, allowing for a maximum radius of three degrees (Schwarz et al., 2018; Figure 1). In the dataset provided here, the geodesic distance between each lake and its paired SSR station is given, as well as the difference in elevation.~~Open source *in situ* surface solar radiation (SSR) data for the period 1950-2020 were collected from stations paired with the selected lakes. Each lake was paired with the closest SSR station using the nearest neighbor function in QGIS, allowing for a maximum radius of three degrees (Schwarz et al., 2018; Figure 1). In the dataset, the geodesic distance between each lake and its paired SSR station is given, as well as the difference in elevation.~~

The SSR data temporal resolution varied from minutes to months. Hence, where needed, the SSR data were resampled to yield monthly mean values. For the Experimental Lakes Area (ELA) in Ontario, Canada, the data were converted from photosynthetically active radiation (PAR) to SSR, where the PAR wavelength range (400-700 nm) was averaged to 550 nm.

2.1.3 Lake characteristics

For each lake, we calculated the trophic status index (TSI) based on the mean chlorophyll-*a* concentration over the sampling period. This TSI value was used to assign the lake to the corresponding trophic state category according to Carlson and Simpson (1996). The HydroLAKES shapefile yielded the lake's surface area, mean depth, and volume (Messager et al., 2016). Lake elevation was extracted from a digital elevation model (DEM) (Danielson and Gesch, 2010), and each lake was assigned its corresponding climate zone using HydroATLAS data (Linke et al., 2019). The reader is referred to the "lake summary" file in the supplementary information for details on the lake characteristics.~~For each lake, we calculated the trophic status index (TSI) based on the mean chlorophyll-*a* concentration over the sampling period. This TSI value was used to assign the lake to the corresponding trophic state category according to Carlson and Simpson (1996). The HydroLAKES shapefile yielded the lake's surface area, mean depth, elevation, and volume (Messager et al., 2016). The climate zone of the lake was extracted from the HydroATLAS shapefile (Linke et al., 2019).~~

2.2 Detecting seasonal periods of chlorophyll-a increase~~growth windows~~

Periods of chlorophyll-*a* increase (PCIs) were identified based on the normalized net rate of change in chlorophyll-*a* concentration (NRCC) at each lake sampling point throughout the year. To locate the start and end of a PCI, we smoothed the annual chlorophyll-*a* time series using a Savitzky-Golay filter (SciPy.signal savgol_filter) and flagged optima in the smoothed data

(SciPy.signal find_peaks) using functions from the open source SciPy ecosystem (Virtanen et al., 2020). The procedure is illustrated in Figure 2.

The NRCC at any given time during the year was calculated by computing the first derivative of the smoothed chlorophyll-*a* concentration versus time and dividing the derivative value by the corresponding chlorophyll-*a* concentration. ~~Growth windows were defined based on the rate of change in chlorophyll-*a* concentration at each lake sampling point throughout the year. To locate the start and end of a growth window, we smoothed the annual chlorophyll-*a* time series using a Savitzky-Golay filter (SciPy.signal savgol_filter) and flagged optima in the smoothed data (SciPy.signal find_peaks) using functions from the open source SciPy ecosystem (Virtanen et al., 2020). The procedure is illustrated in Figure 2.~~

For each lake and each year, the start of the first PCI was defined as the day the NRCC~~spring growth window began when the daily rate of increase~~ surpassed 0.4 day^{-1}. This ~~the~~ threshold rate was selected following a series of sensitivity tests (details provided in the supplementary information). A threshold NRCC value was considered preferable than a threshold RCI value~~0.05 µgL^{-1}day^{-1} for the first time. The 0.05 µgL^{-1}day^{-1} rate was chosen~~ because it accounts for variations among lakes and among years~~corresponds to the median rate at which a distinct switch to a "rapid growth" period~~ in the baseline chlorophyll-*a* concentrations during the non-growing season.

The PCI~~mesotrophic-hypereutrophic lakes in the dataset was observed. The growth window~~ ended on~~at~~ the day the ~~first "~~peak~~"~~ in chlorophyll-*a* concentration was reached, that is, just before the NRCC turned negative. ~~.~~If a threshold NRCC~~rate~~ of 0.4 day~~05 µgL^{-1}day~~$^{-1}$ was not~~never~~ reached during a given year, the PCI~~growth window~~ began when the NRCC~~rate of change~~ first became positive. The second (~~summer (or~~ fall) PCI~~window~~ was identified in the same way, following the end of the first (spring) PCI ~~window~~. If the annual chlorophyll-*a* concentration ~~there was~~ only yielded one peak value in the smoothed data series, only one PCI~~growth window~~ was identified for that year, which~~. This year~~ was then labelled as a "single PCI~~growth window~~" year. ~~(i.e., only one major algal growth window occurred within that year).~~ Years with more than two~~three~~ chlorophyll-*a* peaks~~,~~ or with no peaks~~,~~ were not included in the PCI~~growth window~~ dataset.

Depending on data availability, the pre-PCI period was defined as the one- or two-week period immediately preceding the PCI start day. For each pre-PCI, the mean surface water temperature, SSR, and TP concentration were compiled. These served as simple indicators of how favorable in-lake conditions were to initiate algal growth (Lyngsgaard et al., 2017). An example of a year with a spring and fall PCI is shown in Figure 3. Note that we use the label "fall" to indicate the second yearly PCI, although in some cases the fall PCI was initiated before the fall equinox.

~~Depending on data availability, the pre-growth window was defined as the one or two week period immediately preceding the growth window start date. For each pre-growth window, the mean surface water temperature, SSR, and TP concentration were calculated. These served as (simple) indicators of how favorable in-lake conditions were to initiate algal growth (Lyngsgaard et al., 2017). An example of a spring and summer growth window is shown in Figure 3. Note that we use the label "summer" to indicate the second yearly growth window, although in many cases the summer growth window occurred after the fall equinox.~~

Once the PCI~~growth window~~ and pre-PCI~~growth~~ durations were determined, the mean values of the variables listed in Table 1 were calculated.~~ for both the growth window and the pre-growth window.~~ This was done for each lake and for each year data were available. In the dataset, each row represents a single PCI~~growth window~~ and includes the timing and duration, RCI value, plus the mean values for ~~rate of increase of the chlorophyll-*a* concentration, and~~ all other relevant lake variables, including SSR, averaged for the PCI and pre-PCI.~~.~~ Note that, along with the variables in Table 1, we included the total number of samples collected each year and the mean time between samples. Thus, if desired the user ~~so the dataset~~ can filter the dataset~~be filtered~~ for a higher sampling frequency than done here.~~. The reader is referred to~~ the supplementary information of the dataset also identifies~~included with the dataset for a more detailed explanatory table with additional information on~~ the organization responsible for ~~carrying out the~~ monitoring a given lake~~sampling location~~.

3 Dataset: data distributions

3.1 Dataset characteristics

Most lakes in the dataset are located between 50 and 60° N. The majority of available open data are from organizations within the United Kingdom, Sweden, Canada, and the United States. The years with available data in the dataset are unevenly distributed. The majority of PCIs fall in the period 2005-2019 (Figure 4a), likely due to a combination of increased lake monitoring efforts and a push in recent years towards greater accessibility of publicly funded data (Hallegraeff et al., 2021; Roche et al., 2020). Most sampling frequencies are in the range of 25 to 30 days, with additional peaks at 7 and 14 days (Figure 4b). Thus, with a few exceptions, the PCIs included in the dataset occurred in lakes sampled at a monthly frequency or better. ~~Most lakes in the dataset are located between 50 and 60° N as the majority of available open data are from organizations within the United Kingdom, Sweden, Canada, and the United States. The years with available data in the dataset are unevenly distributed, however, with most detected growth windows falling in the period 2005-2019, likely due to a combination of increased lake monitoring efforts and a push in recent years towards greater accessibility of publicly funded data (Hallegraeff et al., 2021; Roche et al., 2020; Figure 4a).~~

The distribution of trophic states of the PCIs recorded in the dataset are: 1.6% oligotrophic, 18.6% mesotrophic, 75.2% eutrophic, and 4.6% hypereutrophic. Single PCIs dominate oligotrophic lakes where they make up 96.1% of all PCIs (Figure 4c). This may reflect the severe nutrient limitation in oligotrophic lakes, which prevents the occurrence of a second annual algal PCI (Rigosi et al., 2014). Oligotrophic lakes also tend to dominate at latitudes ≥ 55 °N (Figure 4d) where lower water temperatures and lower cumulative solar radiation may further limit algal growth (Lewis, 2011). The PCI durations range from 3 to 275 days, with a median of 68 days (Figure 5a). Fall PCIs tend to be shorter than spring and single PCIs, with the latter exhibiting the most variable start and end days (Figure 5b). ~~The majority of growth windows recorded in the dataset fall in the eutrophic category (1.6% oligotrophic, 18.0% mesotrophic, 75.4% eutrophic, and 5.0% hypereutrophic). Single growth windows dominate oligotrophic lakes where they make up 96% of all growth windows (Figure 4b). This may reflect the severe nutrient limitation in oligotrophic lakes, which prevents the occurrence of a second annual algal growth window (Rigosi et al., 2014). Oligotrophic lakes also tend to occur at the higher latitudes (Figure 4c) where lower water temperatures and solar radiation may further limit algal growth (Lewis, 2011).~~

~~The growth window durations range from 2 to 251 days, with a median of 71 days across all lakes (Figure 5a). Summer growth windows tend to be shorter than those of spring and single growth windows, with the latter exhibiting the most variable start and end dates (Figure 5b).~~

3.2 Environmental conditions during PCIs~~growth windows~~

Rates of chlorophyll-*a* increase during the PCIs exhibit log-normal distributions (Figure 6a). The mean chlorophyll-*a* rate is lowest in the single PCI category and highest in the fall PCIs. Mean surface water temperature has a distinct bimodal spring-fall distribution (Figure 6b). For the single PCIs, the corresponding mean temperatures are evenly distributed across the annual range, which reflects the large spread in the timing of the single PCIs (Figure 5b). Total P concentrations are lowest during the spring PCIs (Figure 6c), consistent with a greater control of P limitation on algal growth during spring compared to summer and fall (Kirillin et al., 2012). Secchi depth during the PCIs ranges from 0.01 to 15.4 m, with fall PCIs experiencing the lowest mean Secchi depth (Figure 6d), as turbidity generally increases after the spring bloom.~~Chlorophyll-*a* rates during the growth windows exhibit log-normal distributions (Figure 6a). The mean chlorophyll-*a* rate is lowest in the single growth window category and highest in the summer growth windows. Mean surface water temperature has a distinct bimodal spring-summer distribution (Figure 6b), which is expected for northern temperate and cold-temperate lakes where surface water temperature during the ice-free period follows the seasonal air temperature trend (Kirillin et al., 2012). For the single growth windows, temperature is evenly distributed across the annual range, which aligns with the large variability in the timing of single growth windows (Figure 5b). Total phosphorus concentrations are lowest during the spring growth windows, which likely reflects a greater control of P limitation on algal growth during spring compared to summer and fall (Kirillin et al., 2012; 6c). Secchi depth during the growth windows ranges from 0.01 to 14.6 m, with summer growth windows experiencing the lowest mean Secchi depth, as turbidity generally increases after the spring bloom (Figure 6d).~~

4 Dataset: examples of trends~~trend analyses~~

The PCI~~growth window~~ delineation and the estimation of RCI~~chlorophyll-*a* rates~~ can in principle be applied to any lake for which time series chlorophyll-*a* concentration data are available. By creating a dataset comprising many lakes and covering multi-year time periods, it becomes possible to extract~~analyze~~ global trends in lake chlorophyll-*a*.~~productivity.~~ Here, we provide a few illustrative examples of how the dataset can be interrogated, ~~thereby~~ setting the stage for its use and extension by other researchers.

4.1 Chlorophyll-*a* rates: trophic status~~, and~~ latitude and climate zone

When grouped by trophic status, mean and median chlorophyll-*a* growth rates (RCIs) show the expected increase from oligotrophic to hypereutrophic lakes (Figure 7a). The rates in the different trophic categories, however, cover ~~very~~ large and overlapping ranges. When grouped according to latitude, lakes between 40 and 50° N exhibit the widest range in RCIs~~chlorophyll-*a* rates~~ (Figure 7b),~~) that,~~ in part due to~~, reflects~~ the high proportion of lakes in this latitude range. The highest latitude lakes (60-70° N) tend to have the lowest RCIs~~chlorophyll-*a* rates~~, which may reflect~~is expected given~~ the cooler temperatures experienced~~and lower solar irradiance they experience~~ (Lewis, 2011~~(Lewis, 2011~~).

The lakes are spread across three climate zones: cold and mesic; cool, temperate, and dry; and warm, temperate, and mesic (Figure 7c). There is considerable overlap in RCI across the climate zones, with no systematic differences in the mean and median RCI values between the zones.

While variations in chlorophyll-*a* rates of increase (RCIs) are often assumed to reflect comparable differences in algal biomass growth rates, it is important to note that the chlorophyll-*a* to biomass ratio varies within and among lakes. In particular, chlorophyll-*a* to biomass ratios are known to be sensitive to variations in solar radiation, temperature, algal species, and cell size (Baumert and Petzodt, 2008; Inomura et al., 2019; Geider, 1987; Álvarez et al., 2017). The summer ratio of chlorophyll-*a* to biomass (the latter typically expressed as particulate organic carbon concentration) generally increases with increasing latitude because algae are adapted to harvest the more variable daylight conditions, including longer summer photoperiods, at higher latitudes (Behrenfeld et al., 2016; Taylor et al., 1997). By contrast, cooler temperatures at higher latitudes may result in higher chlorophyll-*a* to biomass ratios because of lower growth rates, at least when the algae are nutrient-replete (Behrenfeld et al., 2016). Thus, the use of a relative rate (NRCC) as the threshold value for defining a PCI, and as a metric reported in the dataset, facilitates comparisons between lakes of different trophic status or standing stock of chlorophyll-*a*.

~~While differences in chlorophyll-*a* rates usually indicate comparable differences in algal biomass growth rates, it is important to note that the chlorophyll-*a* to biomass ratio varies within and among lakes. In particular, chlorophyll-*a* to biomass ratios are known to be sensitive to variations in solar irradiance and temperature (Behrenfeld et al., 2016). The summer ratio of~~

~~chlorophyll-*a* to biomass (typically expressed as particulate organic carbon concentration) generally decreases with increasing latitude because the algae are adapted to the more variable daylight conditions, including longer summer photoperiods, at higher latitudes (Behrenfeld et al., 2016). By contrast, cooler temperatures at higher latitudes may result in higher chlorophyll-*a* to biomass ratios because of lower growth rates, at least when the algae are nutrient-replete (Behrenfeld et al., 2016).~~

4.2 Chlorophyll-*a* rates: temperature and climate warming

The start and end days~~dates~~ of the spring and~~,~~ single PCIs~~and summer growth windows~~ show temporal trends towards occurrence earlier in the year (Figure 8a). Earlier ~~The trends are most pronounced for the spring windows, which likely reflects a greater sensitivity of~~ springtime algal activity could be linked to global~~climate~~ warming. The latter is expected to result in~~causes~~ earlier ice break-up and ~~produces~~ earlier surface water temperature conditions favorable for algal growth (Markelov et al., 2019). ~~This hypothesis is consistent with the correlations between the chlorophyll-*a* rates and water temperature (Figure 8b).~~

The start and end days~~dates~~ of the spring PCIs~~growth windows~~ show a positive correlation with increasing temperature (Figure 8b). By contrast, little or even negative correlations are seen for the fall PCIs.~~summer growth windows.~~ Thus, all other conditions unchanged, a warmer climate would see earlier spring blooms, but little temporal shifts for the fall PCIs~~summer growth windows~~ and, possibly, even a slight delay. For the spring and single PCIs~~growth windows~~, the duration ~~of the window~~ shows a maximum around 10° C. Therefore, moderate temperatures near or slightly above ~~close to~~ 10° C should, on average, produce the longest lasting algal growth events. The same~~No dinstinct~~ trend is not seen for the fall PCIs, possibly~~summer growth windows, presumably~~ because they occur when water temperatures are already above 10° C.

4.3 Surface~~Chlorophyll-*a* rates:~~ solar ~~irradiance~~

~~Solar~~ radiation **during PCIs: seasonal distributions and distances to lakes**~~is essential for phytoplankton growth (Inomura et al., 2020). For example, at the single lake scale, Tian et al. (2017) showed that SSR is a major predictor of growing-season chlorophyll-*a* concentrations in the Western Basin of Lake Erie. A paleolimnological study of Lake Tanganyika also provided evidence for a positive correlation between multi-centennial oscillations of SSR and diatom~~

~~productivity dating back to ~1000 CE (McGlue et al., 2020). Nonetheless, the relationship between algal growth and SSR has yet to be compared across a large set of lakes.~~

The mean SSR during spring PCIs in the dataset is approximately 100 W m^{-2} (Figure 9), which is lower than the mean SSR values of single and fall PCIs that are both close to 175 W m^{-2}. This difference in mean SSR between spring and fall PCIs is expected, given the longer daylight hours and more intense sunlight experienced in summer and fall compared to early spring. The similarity in mean SSR between single and fall PCIs may be related to the observation that, at higher latitudes (>55°N), single PCIs occur more commonly than double PCIs (Figure 4d). Higher latitude lakes tend to bloom only once during the summer months, taking advantage of the period of the year with the highest SSR (Behrenfeld et al., 2016; Lewis, 2011). In support of this, Figures 5b and 5c show that single PCIs tend to occur between late spring and early fall. On the other hand, at lower latitudes (40-45°N), double PCIs are more common than single PCIs, likely due to higher temperatures and longer periods of sufficient daylight experienced during the spring and fall "shoulder seasons" at these latitudes.

Despite the defining importance of sunlight for photosynthesis, *in situ* SSR time series data are rarely measured systematically as part of lake monitoring programs (Sterner et al., 1997). Although gridded reanalysis datasets that include solar radiation parameters exist, their comparibility with *in situ* SSR measurements remains in question (Wohland et al., 2020). In gathering open source data, we compiled *in situ* SSR measurements from locations as close as possible to the lakes with chlorophyll-*a* data. Nonetheless, much of the SSR values in our dataset were collected at considerable distances from the corresponding lakes (up to ~300 km, Figure 10). For our dataset, only ~10% of the locations where SSR was measured are less than 20 km away from the corresponding lakes, while ~40% are 20-50 km away, ~43% are 50-100 km away, and ~7% are more than 100 km away. Hence, in a significant number of cases, the actual mean SSR during a PCI may differ from the *in situ* mean SSR reported here, due to differences in cloud cover and levels of atmospheric aerosols (among other factors) (Alpert and Kishcha, 2008). Users are therefore advised to consider this limitation when making use of the SSR values in our dataset. Overall, we recognize a need for SSR data to be more systematically measured and reported as part of lake monitoring programs, in particular for oligotrophic lakes.

5Solar radiation is used directly by photosynthetic organisms for carbon fixation (Melkozernov and Blankenship, 2007). In addition, SSR exerts a strong control on lake surface water temperature (Jakkila et al., 2009) and the timing of ice breakup in seasonally ice-covered lakes (Kirillin et al., 2012b), both of which influence lake primary productivity. While the global distribution of mean annual SSR is primarily a function of latitude (Kirillin et al., 2012b), atmospheric controls (e.g., cloud cover) cause regional variability, as well as variability over time (Alpert and Kishcha, 2008; Cutforth and Judiesch, 2007; Wild, 2009). It is important to note that SSR is not related directly to global warming (Kirillin et al., 2012b), nor is it controlled by the cycles in the sun's energy output (Wild, 2009).

To determine to what extent SSR explains variations in chlorophyll-*a* growth rates, we removed the effect of temperature by normalizing the rates using the temperature dependency function (which we refer to as "*ftemp*") proposed by Rosso et al. (1995). This function describes the non-linear temperature dependence of cellular metabolic activity and requires that a minimum, maximum, and optimum growing temperature be assigned. Dividing the *in situ* chlorophyll-*a* rate during the growth window by the corresponding *ftemp* value corrects for the effect of differences in temperature between growth windows.

The temperature-corrected chlorophyll-*a* growth rates indicate that the relationship between SSR and algal growth is a function of the trophic status (i.e., nutrient availability), as seen in Figure 9. Lakes of higher trophic status are more sensitive to SSR than lakes of lower trophic status. For eutrophic lakes, the effect of SSR on the temperature-corrected chlorophyll-*a* rates is most pronounced in the low to moderate SSR range typical of the spring season (Figure 9a). The same effect is not seen when considering the rates without temperature correction (Figure 9b). Thus, the increasing SSR during spring is counterbalanced by cooler temperatures compared to the later summer growth window. Note that the summer chlorophyll-*a* growth rates show little influence from SSR, whether corrected or not for temperature, supporting the theory of a greater top-down control on algal growth during the summer versus the spring as proposed, among others, by Lyngsgaard et al. (2017).

The chlorophyll-*a* growth rate data near or above 200 Wm^{-2} remain low, with no clear dependence on SSR. This is likely indicative of a photoacclimation response of the algae, where they produce less chlorophyll-*a* in proportion to their total biomass so they can allocate more

~~resources to growth when nutrients – not light – are limiting growth (Lewis et al., 2018; Inomura et al., 2020). Furthermore, when light intensity during the summer months reaches damaging levels, algae may start producing additional photosynthetic pigments to protect their chlorophyll (so-called sunscreen pigments). However, nutrient availability may limit the amount of pigments that can be synthesized, impeding the photoacclimation response (Lewis et al., 2018). This nutrient limitation of the photoacclimation response would explain the differences in the temperature corrected growth rate's sensitivity to SSR as a function of trophic status (Figure 9a). Lakes of higher trophic status (i.e., less nutrient limitation) show a larger response to changes in SSR, presumably because they have sufficient nutrients to produce additional chlorophyll-*a* in response to an increase in SSR.~~

~~5 Key findings~~

~~The following points summarize the general trends that emerged from our analysis of the dataset.~~

1. ~~Higher water temperatures and reduced ice-cover cause algal growth windows to start earlier in the year, extending the growing season and potentially increasing annual net primary productivity of northern lakes under ongoing and future climate warming.~~
2. ~~Chlorophyll-*a* growth rates increase with nutrient availability while they decrease at higher latitudes due to cooler temperatures and lower SSR.~~
3. ~~Oligotrophic lakes tend to have the highest proportion of single annual growth windows, likely reflecting the dominant role of nutrient limitation.~~
4. ~~Temperature-corrected chlorophyll-*a* growth rates suggest a relationship with SSR that depends on the trophic state of lakes:~~
    a. ~~compared to mesotrophic and oligotrophic lakes, eutrophic lakes exhibit a higher sensitivity to SSR, especially in the low to moderate irradiance levels experienced during spring;~~
    b. ~~at the upper end of SSR, chlorophyll-*a* growth rates remain low and independent of SSR, which may reflect a photoacclimation response of algae.~~
5. ~~The low SSR sensitivity of chlorophyll-*a* growth rates during summer and fall suggests a stronger top-down control on algal growth compared to the earlier spring growth windows.~~

~~6. In summary, light limitation is an important control on chlorophyll-*a* growth rates during spring, whereas lower nutrient availability and increased grazing from zooplankton tend to be more significant during summer.~~

~~6~~ Conclusions

We present a novel way to delineate annual periods of chlorophyll-*a* increase (PCIs) in lakes that, presumably, overlap with periods of algal growth. We apply this approach to derive the chlorophyll-*a* rates of increase (RCIs) during the PCIs of 343 lakes from cold and cold-temperate regions in the northern hemisphere and covering the period 1964-2019. The derived RCIs are assembled in an open-source dataset, together with additional information on the lakes, including water quality, trophic state, and surface solar radiation. Note that the dataset can be paired with other databases, such as HydroLAKES (Messager et al., 2016), HydroATLAS (Linke et al., 2019), and GLCP (Meyer et al., 2020), to access additional lake and/or watershed attributes. Our dataset is designed to support comparative analyses of the controls on lake chlorophyll-*a* dynamics and, by extension, also algal dynamics, within and between lakes. We present several examples of such analyses. We hope these will encourage others to use the dataset in their own research and to further expand the dataset's geographical reach and information content. ~~We present a novel way to delineate periods of rapid algal growth, or growth windows, in lakes based on time series chlorophyll-*a* measurements. We apply this approach to derive the chlorophyll-*a* growth rates occurring during the growth windows of 357 lakes from cold and cold-temperate regions in the northern hemisphere, using data collected between 1964 and 2019. The derived growth rates are assembled in an open-source dataset, together with additional information on the lakes including data on water quality, trophic state, and solar radiation. Note that the dataset can be paired with databases such as the~~ **Error! Hyperlink reference not valid.**~~,~~ **Error! Hyperlink reference not valid.** ~~and~~ **Error! Hyperlink reference not valid.** ~~databases to access additional lake and/or watershed attributes. Our dataset is designed to support comparative analyses of the controls on algal productivity within and between lakes. We present several examples of such analyses. We hope these will encourage others to use the dataset in their own research and to further expand the dataset's geographical reach and information content.~~

Code and data availability

All code is available in the project GitHub repository (https://github.com/hfadams/growth_window) and in Zenodo (https://doi.org/10.5281/zenodo.5171442). The PCI~~growth window~~ dataset and supplementary data files can be openly accessed at~~are available in~~ the Federated Research Data Repository at https://doi.org/10.20383/102.0488 (Adams et al., 2021)~~(Adams et al., 2021)~~.

Author contributions

All authors took part in development of the study. SS, BP, ~~HKP~~ and PVC~~HKP~~ conceptualized the study, while HA and JY developed the methods and carried out the data collection and data post-processing. HA wrote the original manuscript with contributions from JY, BP, SS, HKP, and PVC. All authors reviewed and edited the final paper.

Competing interests

The authors declare that they have no conflict of interest.

Acknowledgments

This work was~~is~~ funded by the Lake Futures project within the Global Water Futures (GWF) project supported by the Canada First Research Excellence Fund (CFREF).~~Fund's Global Water Futures Programme.~~ We would ~~also~~ like to thank all the institutions and authors listed in the supplementary information for making their data open source and free to support our work.~~this research.~~

References

Adams, H., Ye, J., Slowinski, S., Persaud, B., Kheyrollah Pour, H., and Van Cappellen, P.: Chlorophyll-a growth rates and related environmental variables in global temperate and cold-temperate lakes, Fed. Res. Data Repos., https://doi.org/https://doi.org/10.20383/102.0488, 2021.

Allen, M., Poggiali, D., and Whitaker, K.: Raincloud plots: a multi-platform tool for robust data visualization [version 2; peer review: 2 approved], Wellcome Open Res, 4, https://doi.org/https://doi.org/10.12688/wellcomeopenres.15191.2, 2021.

Álvarez, E., Nogueira, E., and López-Urrutia, Á.: In vivo single-cell fluorescence and size scaling of phytoplankton chlorophyll content, Appl. Environ. Microbiol., 83, https://doi.org/10.1128/AEM.03317-16/SUPPL_FILE/ZAM999117731S1.PDF, 2017.

Battin, T. J., Kaplan, L. A., Findlay, S., Hopkinson, C. S., Marti, E., Packman, A. I., Newbold, J. D., and Sabater, F.: Biophysical controls on organic carbon fluxes in fluvial networks, Nat. Geosci., 1, 95–100, https://doi.org/10.1038/ngeo101, 2008.

Baumert, H. Z. and Petzodt, T.: The role of temperature, cellular quota and nutrient concentrations for photosynthesis, growth and light-dark acclimation in phytoplankton, 38, 313–326, https://doi.org/10.1016/J.LIMNO.2008.06.002, 2008.

Behrenfeld, M. J., O'Malley, R. T., Boss, E. S., Westberry, T. K., Graff, J. R., Halsey, K. H., Milligan, A. J., Siegel, D. A., and Brown, M. B.: Revaluating ocean warming impacts on global phytoplankton, Nat. Clim. Chang., 6, 323–330, https://doi.org/10.1038/nclimate2838, 2016.

Carlson, R. E. and Simpson, J.: A coordinator's guide to volunteer lake monitoring methods., North Am. Lake Manag. Soc., 96, 1996.

Carpenter, S. R., Kitchell, J. F., Hodgson, J. R., Carpenter, S. R., Kitchell, J. F., and Hodgson, J. R.: Cascading trophic interactions and lake productivity, 35, 634–639, 2016.

Codd, G. A., Morrison, L. F., and Metcalf, J. S.: Cyanobacterial toxins: Risk management for health protection, Toxicol. Appl. Pharmacol., 203, 264–272, https://doi.org/10.1016/j.taap.2004.02.016, 2005.

Cole, J., J., Prarie, Y. T., Caraco, N. F., McDowel, L. T., Tranvik, L. J., Striegel, C. M., Duarte, C. M., Kortelainen, P., Downing, J. A., Middleburg, J. J., and Melack, J.: Plumbing the Global Carbon Cycle: Integrating Inland Waters into the Terrestrial Carbon Budget, 10, 171–184, https://doi.org/10.1007/s, 2007.

Creed, I. F., Bergström, A. K., Trick, C. G., Grimm, N. B., Hessen, D. O., Karlsson, J., Kidd, K. A., Kritzberg, E., McKnight, D. M., Freeman, E. C., Senar, O. E., Andersson, A., Ask, J., Berggren, M., Cherif, M., Giesler, R., Hotchkiss, E. R., Kortelainen, P., Palta, M. M., Vrede, T., and Weyhenmeyer, G. A.: Global change-driven effects on dissolved organic matter composition: Implications for food webs of northern lakes, Glob. Chang. Biol., 24, 3692–3714, https://doi.org/10.1111/gcb.14129, 2018.

Danielson, J. and Gesch, D.: Global Multi-resolution terrain elevation data 2010 (GMTED2010), U.S. Geol. Surv. open-file Rep., 26, 2011–1073, 2010.

Deng, J., Paerl, H. W., Qin, B., Zhang, Y., Zhu, G., Jeppesen, E., Cai, Y., and Xu, H.: Climatically-modulated decline in wind speed may strongly affect eutrophication in shallow lakes, Sci. Total Environ., 645, 1361–1370, https://doi.org/10.1016/j.scitotenv.2018.07.208, 2018.

Dorset Environmental Science Centre: Lakeshore Capacity Assessment Handbook: Protecting Water Quality in Inland Lakes on Ontario’s Precambrian Shield Appendix C, Dorset Environmental Science Centre Technical Bulletins., Toronto, Ontario, 2010.

Downing, J. A., Prarie, Y. T., Cole, J., J., Duarte, C. M., Tranvik, L. J., Striegl, R. G., McDowell, W. H., Kortelainen, P., Caraco, N. F., Melack, J., M., and Middelburg, J. J.: The global abundance and size distribution of lakes, ponds and impoundments, Limnol. Oceanogr., 51, 2388–2397, https://doi.org/10.1016/B978-012370626-3.00025-9, 2006.

Geider, R. J.: Light and Temperature Dependence of the Carbon to Chlorophyll a Ratio in Microalgae and Cyanobacteria: Implications for Physiology and Growth of Phytoplankton, New Phytol., 1–34, 1987.

German, A., Tauro, C., Scavuzzo, M. C., and Ferral, A.: Detection of algal blooms in a eutrophic reservoir based on chlorophyll-a time series data from MODIS, Int. Geosci. Remote Sens. Symp., 2017-July, 4008–4011, https://doi.org/10.1109/IGARSS.2017.8127879, 2017.

Gleick, P.: Water and conflict, Int. Secur., 18, 112, https://doi.org/10.1016/S0262-4079(13)60875-1, 1993.

Hallegraeff, G. M., Anderson, D. M., Belin, C., Bottein, M.-Y. D., Bresnan, E., Chinain, M., Enevoldsen, H., Iwataki, M., Karlson, B., McKenzie, C. H., Sunesen, I., Pitcher, G. C., Provoost, P., Richardson, A., Schweibold, L., Tester, P. A., Trainer, V. L., Yñiguez, A. T., and Zingone, A.: Perceived global increase in algal blooms is attributable to intensified monitoring and emerging bloom impacts, Commun. Earth Environ., 2, https://doi.org/10.1038/s43247-021-00178-8, 2021.

Hampton, S. E., Galloway, A. W. E., Powers, S. M., Ozersky, T., Woo, K. H., Batt, R. D., Labou, S. G., O’Reilly, C. M., Sharma, S., Lottig, N. R., Stanley, E. H., North, R. L., Stockwell, J. D., Adrian, R., Weyhenmeyer, G. A., Arvola, L., Baulch, H. M., Bertani, I., Bowman, L. L., Carey, C. C., Catalan, J., Colom-Montero, W., Domine, L. M., Felip, M., Granados, I., Gries, C., Grossart, H. P., Haberman, J., Haldna, M., Hayden, B., Higgins, S. N., Jolley, J. C., Kahilainen, K. K., Kaup, E., Kehoe, M. J., MacIntyre, S., Mackay, A. W., Mariash, H. L., McKay, R. M., Nixdorf, B., Nõges, P., Nõges, T., Palmer, M., Pierson, D. C., Post, D. M., Pruett, M. J., Rautio, M., Read, J. S., Roberts, S. L., Rücker, J., Sadro, S., Silow, E. A., Smith, D. E., Sterner, R. W., Swann, G. E. A., Timofeyev, M. A., Toro, M., Twiss, M. R., Vogt, R. J., Watson, S. B., Whiteford, E. J., and Xenopoulos, M. A.: Ecology under lake ice, Ecol. Lett., 20, 98–111, https://doi.org/10.1111/ELE.12699, 2017.

Harris, C. R., Millman, K. J., van der Walt, S. J., Gommers, R., Virtanen, P., Cournapeau, D., Wieser, E., Taylor, J., Berg, S., Smith, N. J., Kern, R., Picus, M., Hoyer, S., van Kerkwijk, M. H., Brett, M., Haldane, A., del Río, J. F., Wiebe, M., Peterson, P., Gérard-Marchant, P., Sheppard, K., Reddy, T., Weckesser, W., Abbasi, H., Gohlke, C., and Oliphant, T. E.: Array programming with NumPy, https://doi.org/10.1038/s41586-020-2649-2, September 2020.

Henderson-Seller, B. and Markland, H. R.: Decaying Lakes—The Origins and Control of Cultural

Eutrophication, New York, NY, 1987.

Huisman, J. and Hulot, F. D.: Population Dynamics of Harmful Cyanobacteria, 143–176, https://doi.org/10.1007/1-4020-3022-3_7, 2005.

Huot, Y., Babin, M., Bruyant, F., Grob, C., Twardowski, M. S., and Claustre, H.: Relationship between photosynthetic parameters and different proxies of phytoplankton biomass in the subtropical ocean, 4, 853–868, https://doi.org/10.5194/bg-4-853-2007, 2007.

Inomura, K., Deutsch, C., Wilson, S. T., Masuda, T., Lawrenz, E., Bučinská, L., Sobotka, R., Gauglitz, J. M., Saito, M. A., Prášil, O., and Follows, M. J.: Quantifying Oxygen Management and Temperature and Light Dependencies of Nitrogen Fixation by Crocosphaera watsonii, 4, https://doi.org/10.1128/MSPHERE.00531-19/SUPPL_FILE/MSPHERE.00531-19-ST002.PDF, 2019.

Jeppesen, E., Søndergaard, M., and Jensen, J. P.: Climatic warming and regime shifts in lake food webs - Some comments, Limnol. Oceanogr., 48, 1346–1349, https://doi.org/10.4319/lo.2003.48.3.1346, 2003.

Jeppesen, E., Canfield, D. E., Bachmann, R. W., Søndergaard, M., Havens, K. E., Johansson, L. S., Lauridsen, T. L., Sh, T., Rutter, R. P., Warren, G., Ji, G., and Hoyer, M. V.: Toward predicting climate change effects on lakes: a comparison of 1656 shallow lakes from Florida and Denmark reveals substantial differences in nutrient dynamics, metabolism, trophic structure, and top-down control, Inl. Waters, 10, 197–211, https://doi.org/10.1080/20442041.2020.1711681, 2020.

Jonsson, P. R., Pavia, H., and Toth, G.: Formation of harmful algal blooms cannot be explained by allelopathic interactions, Proc. Natl. Acad. Sci. U. S. A., 106, 11177–11182, https://doi.org/10.1073/pnas.0900964106, 2009.

Kirillin, G., Leppäranta, M., Terzhevik, A., Granin, N., Bernhardt, J., Engelhardt, C., Efremova, T., Golosov, S., Palshin, N., Sherstyankin, P., Zdorovennova, G., and Zdorovennov, R.: Physics of seasonally ice-covered lakes: A review, Aquat. Sci., 74, 659–682, https://doi.org/10.1007/s00027-012-0279-y, 2012.

Lauerwald, R., Regnier, P., Figueiredo, V., Enrich-Prast, A., Bastviken, D., Lehner, B., Maavara, T., and Raymond, P.: Natural Lakes Are a Minor Global Source of N2O to the Atmosphere, Global Biogeochem. Cycles, 33, 1564–1581, https://doi.org/10.1029/2019GB006261, 2019.

Lewis, K. M., Arntsen, A. E., Coupel, P., Lowry, K. E., Dijken, G. L. Van, Selz, V., Arrigo, K. R., Matsuoka, A., and Mills, M. M.: Photoacclimation of Arctic Ocean phytoplankton to shifting light and nutrient limitation, 1–18, https://doi.org/10.1002/lno.11039, 2018.

Lewis, W.: Global primary production of lakes: 19th Baldi Memorial Lecture, Inl. Waters, 1, 1–28, https://doi.org/10.5268/iw-1.1.384, 2011.

Linke, S., Lehner, B., Ouellet Dallaire, C., Ariwi, J., Grill, G., Anand, M., Beames, P., Burchard-Levine, V., Maxwell, S., Moidu, H., Tan, F., and Thieme, M.: Global hydro-environmental sub-basin and river reach characteristics at high spatial resolution, Sci. Data, 6, 1–15, https://doi.org/10.1038/s41597-019-0300-6, 2019.

Lyngsgaard, M. M., Markager, S., Richardson, K., Møller, E. F., and Jakobsen, H. H.: How Well Does Chlorophyll Explain the Seasonal Variation in Phytoplankton Activity?, 40, 1263–1275, https://doi.org/10.1007/s12237-017-0215-4, 2017.

Markelov, I., Couture, R. M., Fischer, R., Haande, S., and Van Cappellen, P.: Coupling Water Column and Sediment Biogeochemical Dynamics: Modeling Internal Phosphorus Loading, Climate Change Responses, and Mitigation Measures in Lake Vansjø, Norway, J. Geophys. Res. Biogeosciences, 124, 3847–3866, https://doi.org/10.1029/2019JG005254, 2019.

Messager, M. L., Lehner, B., Grill, G., Nedeva, I., and Schmitt, O.: Estimating the volume and age of water stored in global lakes using a geo-statistical approach, Nat. Commun., 7, 1–11, https://doi.org/10.1038/ncomms13603, 2016.

O'Beirne, M. D., Werne, J. P., Hecky, R. E., Johnson, T. C., Katsev, S., and Reavie, E. D.: Anthropogenic climate change has altered primary productivity in Lake Superior, Nat. Commun., 8, 15713, https://doi.org/10.1038/ncomms15713, 2017.

O'Connell, D. W., Ansems, N., Kukkadapu, R. K., Jaisi, D., Orihel, D. M., Cade-Menun, B. J., Hu, Y., Wiklund, J., Hall, R. I., Chessell, H., Behrends, T., and Van Cappellen, P.: Changes in Sedimentary Phosphorus Burial Following Artificial Eutrophication of Lake 227, Experimental Lakes Area, Ontario, Canada, J. Geophys. Res. Biogeosciences, 125, https://doi.org/10.1029/2020JG005713, 2020.

Python Software Foundation: Python Language, 2021.

QGIS.org: QGIS Geographic Information System, 2021.

Reback, J., McKinney, W. jbrockmendel, Van den Bossche, J., Augspurger, T., Cloud, P., Gfyoung, Sinhrks, Klein, A., Roeschke, M., Hawkins, S., Tratner, J., She, C., Ayd, W., Petersen, T., Garcia, M., Schendel, J., and Hayden, A.: pandas-dev/pandas: Pandas 1.0.3 (v1.0.3), 2020.

Riederer, C.: Dplython, 2015.

Rigosi, A., Carey, C. C., Ibelings, B. W., and Brookes, J. D.: The interaction between climate warming and eutrophication to promote cyanobacteria is dependent on trophic state and varies among taxa, Limnol. Oceanogr., 59, 99–114, https://doi.org/10.4319/lo.2014.59.1.0099, 2014.

Roche, D. G., Granados, M., Austin, C. C., Wilson, S., and Mitchell, G. M.: Open government data and environmental science : a federal Canadian perspective, 942–962, https://doi.org/10.1139/facets-2020-0008, 2020.

Rouse, W. R., Douglas, M. S., Hecky, R. E., Hershey, A. E., King, G. W., Lesack, L., Marsh, P., McDonald, M., Nicholson, B. J., Roulet, N. T., and Smol, J. P.: Effects of climate change on the freshwaters of arctic and subarctic North America, Hydrol. Process., 11, 873–902, 1997.

Rousseaux, C. S. and Gregg, W. W.: Interannual variation in phytoplankton primary production at a global scale, Remote Sens., 6, 1–19, https://doi.org/10.3390/rs6010001, 2013.

Schindler, D. W.: A Hypothesis to Explain Differences and Similarities Among Lakes in the Experimental Lakes Area, Northwestern Ontario, J. Fish. Res. Board Canada, 28, 295–301, https://doi.org/10.1139/f71-039, 1971.

Schwarz, M., Folini, D., Hakuba, M. Z., and Wild, M.: From Point to Area: Worldwide Assessment of the Representativeness of Monthly Surface Solar Radiation Records, J. Geophys. Res. Atmos., 123, 13,857-13,874, https://doi.org/10.1029/2018JD029169, 2018.

Sommer, U., Gliwicz, Z. M., Lampert, W., and Duncan, A.: The PEG-model of seasonal succession of planktonic events in fresh waters, Arch. für Hydrobiol., 106, 433–471, 1986.

Sterner, R. W., Elser, J. J., Fee, E. J., Guildford, S. J., and Chrzanowski, T. H.: The light: Nutrient ratio in lakes: The balance of energy and materials affects ecosystem structure and process, Am. Nat., 150, 663–684, 1997.

Tett, P.: The ecophysiology of exceptional blooms, Rapp. Proces-verbaux des Reun. Cons. Int. pour l'Exploration la Mer, 3, 47–60, 1987.

Tranvik, L. J., Downing, J. A., Cotner, J. B., Loiselle, S. A., Striegl, R. G., Ballatore, T. J., Dillon, P., Finlay, K., Fortino, K., Knoll, L. B., Kortelainen, P. L., Kutser, T., Larsen, S., Laurion, I., Leech, D. M., Leigh McCallister, S., McKnight, D. M., Melack, J. M., Overholt, E., Porter, J. A., Prairie, Y., Renwick, W. H., Roland, F., Sherman, B. S., Schindler, D. W., Sobek, S., Tremblay, A., Vanni, M. J., Verschoor, A. M., Von Wachenfeldt, E., and Weyhenmeyer, G. A.: Lakes and reservoirs as regulators of carbon cycling and climate, Limnol. Oceanogr., 54, 2298–2314, https://doi.org/10.4319/lo.2009.54.6_part_2.2298, 2009.

United States Environmental Protection Agengy: 2012 National Lakes Assessment. Field Operations Manual., Washington, DC, EPA 841-B-11-003. pp., 2012.

Verpoorter, C., Kutser, T., Seekell, D., and Tranvik, L.: A global inventory of lakes based on high-resolution satellite imagery, Geophys. Res. Lett., 41, 6396–6402, https://doi.org/10.1002/2014GL060641.Received, 2014.

Virtanen, P., Gommers, R., Oliphant, T. E., Haberland, M., Reddy, T., Cournapeau, D., Burovski, E., Peterson, P., Weckesser, W., Bright, J., van der Walt, S. J., Brett, M., Wilson, J., Millman, K. J., Mayorov, N., Nelson, A. R. J., Jones, E., Kern, R., Larson, E., Carey, C. J., Polat, İ., Feng, Y., Moore, E. W., VanderPlas, J., Laxalde, D., Perktold, J., Cimrman, R., Henriksen, I., Quintero, E. A., Harris, C. R., Archibald, A. M., Ribeiro, A. H., Pedregosa, F., van Mulbregt, P., Vijaykumar, A., Bardelli, A. Pietro, Rothberg, A., Hilboll, A., Kloeckner, A., Scopatz, A., Lee, A., Rokem, A., Woods, C. N., Fulton, C., Masson, C., Häggström, C., Fitzgerald, C., Nicholson, D. A., Hagen, D. R., Pasechnik, D. V., Olivetti, E., Martin, E., Wieser, E., Silva, F., Lenders, F., Wilhelm, F., Young, G., Price, G. A., Ingold, G. L., Allen, G. E., Lee, G. R., Audren, H., Probst, I., Dietrich, J. P., Silterra, J., Webber, J. T., Slavič, J., Nothman, J., Buchner, J., Kulick, J., Schönberger, J. L., de Miranda Cardoso, J. V., Reimer, J., Harrington, J., Rodríguez, J. L. C., Nunez-Iglesias, J., Kuczynski, J., Tritz, K., Thoma, M., Newville, M., Kümmerer, M., Bolingbroke, M., Tartre, M., Pak, M., Smith, N. J., Nowaczyk, N., Shebanov, N., Pavlyk, O., Brodtkorb, P. A., Lee, P., McGibbon, R. T., Feldbauer, R., Lewis, S., Tygier, S., Sievert, S., Vigna, S., Peterson, S., More, S., Pudlik, T., et al.: SciPy 1.0: fundamental algorithms for scientific computing in Python, Nat. Methods, 17, 261–272, https://doi.org/10.1038/s41592-019-0686-2, 2020.

QGIS Development Team.: QGIS Geographic information system, 2021.

Watson, S. B., Miller, C., Arhonditsis, G., Boyer, G. L., Carmichael, W., Charlton, M. N., Confesor, R., Depew, D. C., Höök, T. O., Ludsin, S. A., Matisoff, G., McElmurry, S. P., Murray, M. W., Peter Richards, R., Rao, Y. R., Steffen, M. M., and Wilhelm, S. W.: The re-eutrophication of Lake Erie: Harmful algal blooms and hypoxia, Harmful Algae, 56, 44–66, https://doi.org/10.1016/j.hal.2016.04.010, 2016.

Wetzel, R. G.: Limnology: Lake and River Ecosystems, third edition, Academic press, 2001.

Williamson, C. E., Saros, J. E., Vincent, W. F., and Smol, J. P.: Lakes and reservoirs as sentinels, integrators, and regulators of climate change, Limnol. Oceanogr., 54, 2273–2282, https://doi.org/10.4319/LO.2009.54.6_PART_2.2273, 2009.

Wohland, J., Brayshaw, D., Bloomfield, H., and Wild, M.: European multidecadal solar variability badly captured in all centennial reanalyses except CERA20C, Environ. Res. Lett., 15, 104021, https://doi.org/10.1088/1748-9326/ABA7E6, 2020.

Woolway, R. I. and Merchant, C. J.: Worldwide alteration of lake mixing regimes in response to climate change, Nat. Geosci. |, 12, 271–276, https://doi.org/10.1038/s41561-019-0322-x, 2019.

Zohary, T., Padisák, J., and Naselli-Flores, L.: Phytoplankton in the physical environment: beyond nutrients, at the end, there is some light, Hydrobiol. 2009 6391, 639, 261–269, https://doi.org/10.1007/S10750-009-0032-2, 2009.

Table 1: Summary of variables in the PCI dataset. Associated lake data (e.g., lake depth, surface area, volume, climate zone) are available in the supplementary information.

~~*Table 1: Summary of variables in the derived growth window dataset.*~~

Variable	Units	Description	Comments
Timing	NA	Three possible PCIs: spring, fall, or single PCI	A single PCI occurs when there is only one maximum in the smoothed yearly chlorophyll-*a* concentration time series for the year
Period of chlorophyll-*a* increase (PCI) start day		Day of year when the PCI begins	
Period of chlorophyll-*a* increase (PCI) end day		Day of year when the PCI ends	
Rate of chlorophyll-*a* increase (RCI)	µg L^{-1} day^{-1}	Difference in chlorophyll-*a* concentration between start and end of the PCI divided by the duration of the PCI	One RCI value is associated with each PCI
Normalized rate of change in chlorophyll-*a* (NRCC)	day^{-1}	RCI divided by the initial chlorophyll-*a* concentration	Accounts for variable standing stock of chlorophyll-*a*
Rate of particulate organic carbon (POC) increase	mg L^{-1} day^{-1}	Same calculation as RCI but using start and end POC concentrations	Proxy for the rate of change in total algal biomass
RCI:rate of POC increase	mg chlorophyll-*a* mg^{-1} POC		Accounts for variable chlorophyll-*a* content of algal biomass
Mean PCI surface water temperature	°C	Mean value during the PCI and the 14-day pre-PCI	
Mean PCI surface solar radiation	W m^{-2}	Mean value during the PCI and the 14-day pre-PCI	
Mean PCI total phosphorus (TP)	mg L^{-1}		(Co-)limiting macronutrients
Mean PCI soluble reactive phosphorus (SRP)	mg L^{-1}	Mean values during the PCI	
Mean PCI total Kjeldahl nitrogen (TKN)	mg L^{-1}		
Mean PCI Secchi depth	m		Proxy for turbidity
Mean PCI pH	pH units		
Trophic Status Index (TSI)	Range: 0-100	Calculated from chlorophyll-*a* concentrations across all years the lake was sampled	Basis for assigning trophic status
Trophic status	NA	Trophic status class assigned based on TSI: Oligotrophic, Mesotrophic, Eutrophic, or Hypereutrophic	TSI thresholds are those of the North American Lake Management Society

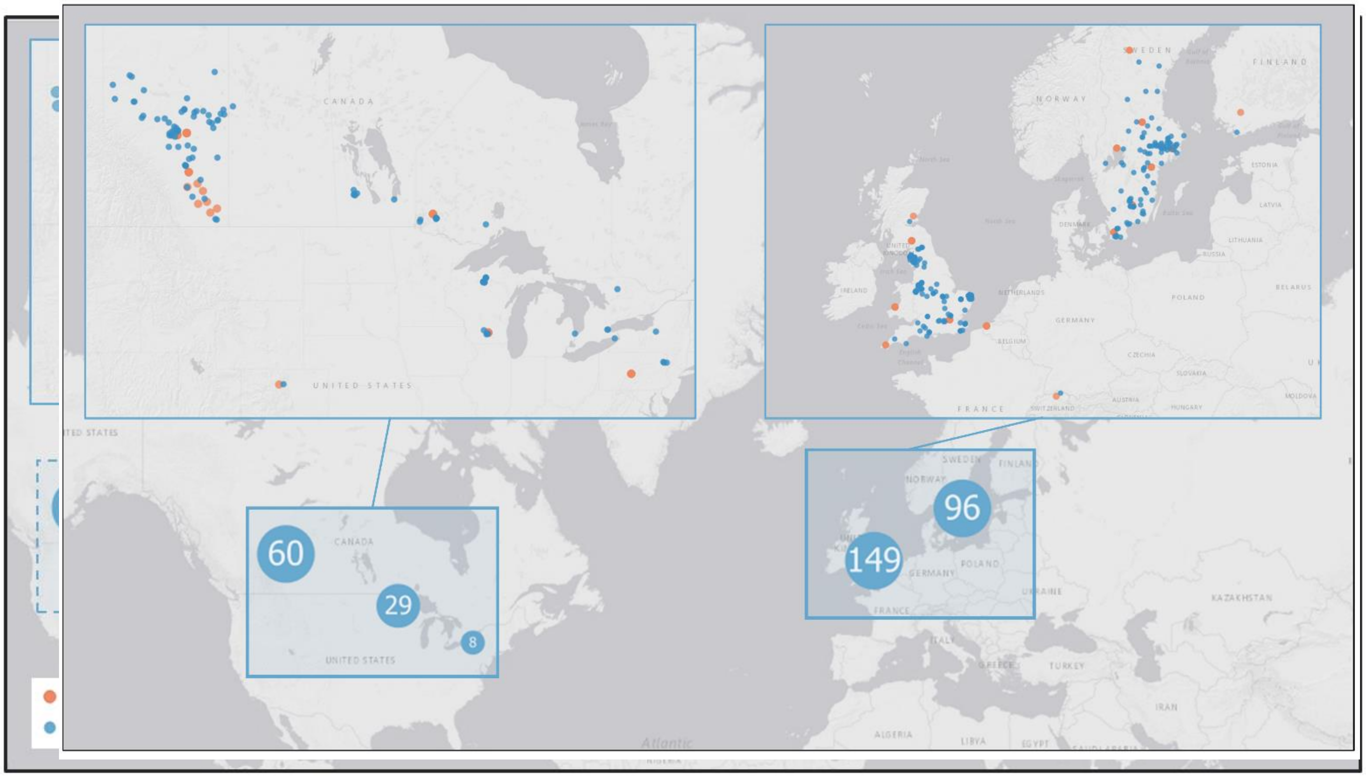

Figure 1: Distribution of the 343~~357~~ lake sampling locations in the PCI~~growth window~~ dataset. Lake Sampling points are clustered by proximity, where marker size and value indicate the number of unique locations represented by each point (light blue markers with white text).~~.~~ Enlarged sections show each lake sampling location (blue markers) and along with the location of the 320~~322~~ paired SSR stations (orange markers).~~.~~ Base map credit: ESRI, 2011.

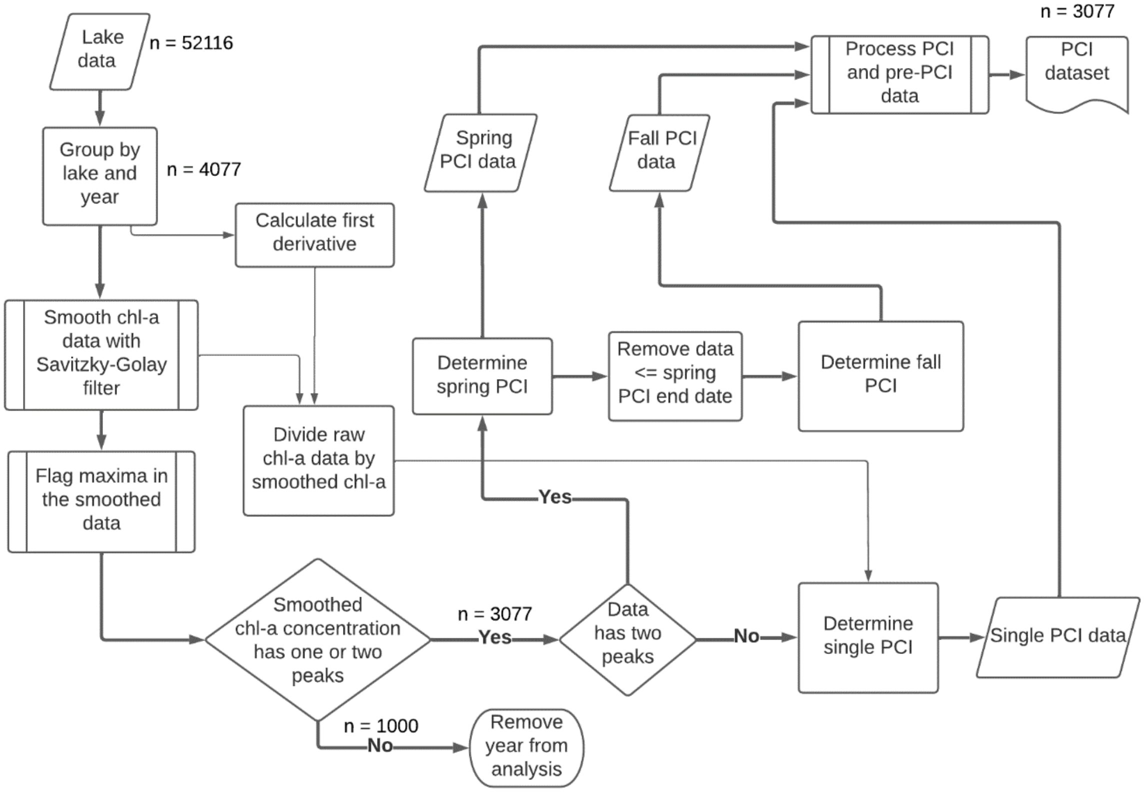
Lake data
n = 52116
Group by lake and year
n = 4077
Calculate first derivative
Smooth chl-a data with Savitzky-Golay filter
Divide raw chl-a data by smoothed chl-a
Flag maxima in the smoothed data
Smoothed chl-a concentration has one or two peaks
n = 3077
Yes
n = 1000
No
Remove year from analysis
Data has two peaks
Yes
No
Determine spring PCI
Remove data <= spring PCI end date
Determine fall PCI
Spring PCI data
Fall PCI data
Determine single PCI
Single PCI data
Process PCI and pre-PCI data
n = 3077
PCI dataset

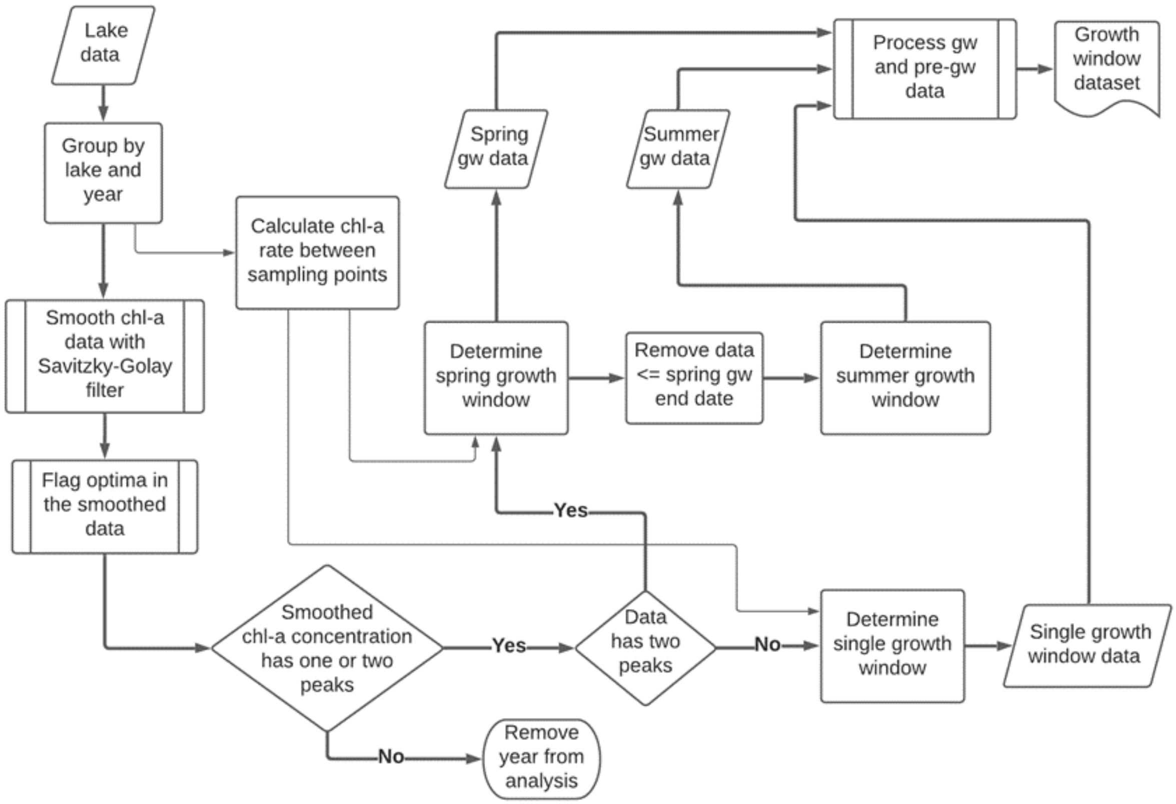

Figure 2: Workflow for detecting PCIs and processing ~~growth window~~ data. For each lake sampling point, chlorophyll-a (Chl-a) data are smoothed with a Savitzky-Golay filter and then PCIs~~growth windows~~ are detected based on peaks in the chlorophyll-a concentration. PCIs~~Growth windows~~ are flagged as spring, fall~~summer~~, or single PCIs. The data density is shown at key points along the workflow~~growth windows~~.

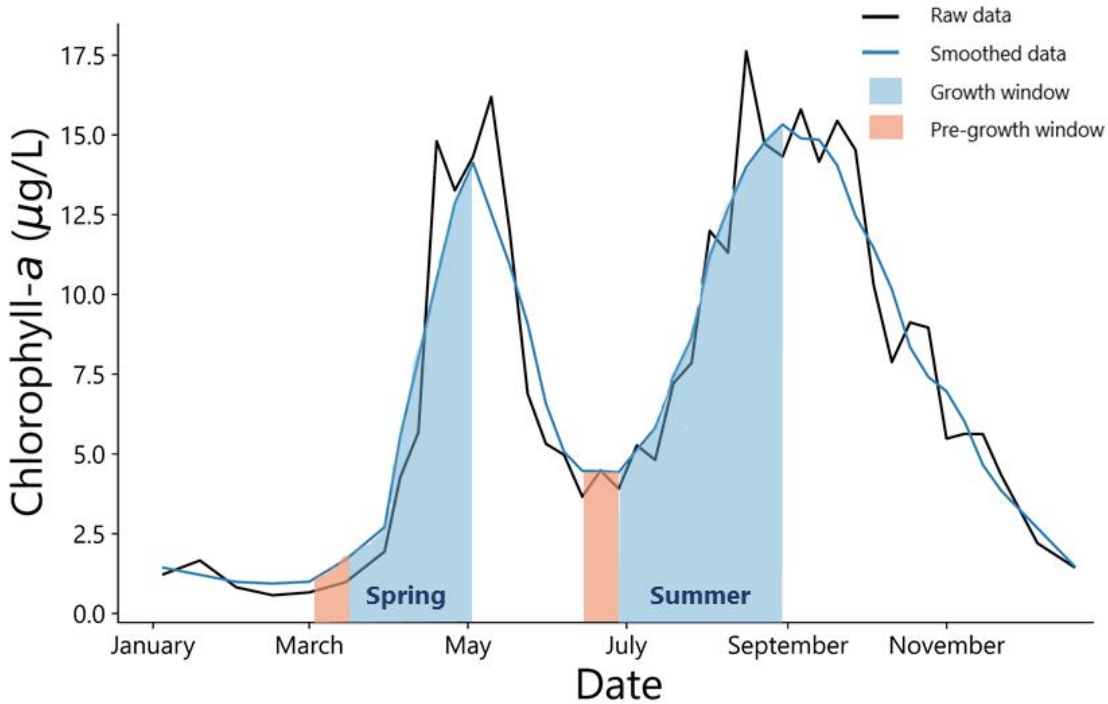

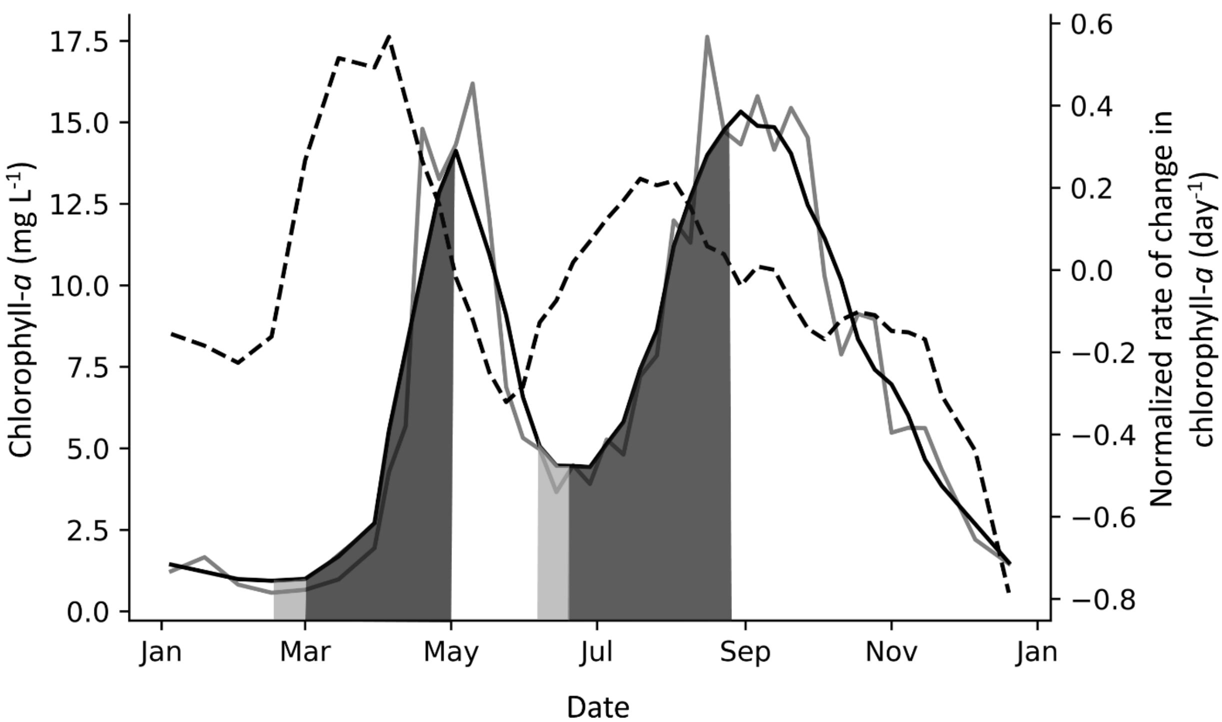

Figure 3. Example of spring and fall PCIs~~summer growth windows~~ in Lake Windermere's north basin in 1988. The solid grey line is ~~Peaks in~~ the ~~smoothed data indicate the end of the growth window, and the window begins when the rate of increase in~~

chlorophyll-a concentration (µg L $^{-1}$), and the solid black line is the chlorophyll-a concentration smoothed with a Savitzky-Golay filter. The dashed line is the normalized rate of change in chlorophyll-a (NRCC) (day^{-1}) where the first derivative is divided by the smoothed chlorophyll-a concentration and is plotted using the right axis. The PCI begins when the NRCC surpasses a threshold of 0.4 day^{-1} as shown in the first (spring) PCI and ends when the NRCC turns negative, which is when the peak chlorophyll-a concentration is reached. When a peak is detected but the NRCC does not surpass a threshold of 0.4 day^{-1}, the PCI begins when the NRCC surpasses 0 day^{-1} as shown in the second (fall) PCI. The PCI~~05 µgL^{-1}day^{-1} (median rate for the distinct switch to a "rapid growth" period in mesotrophic-hypereutrophic lakes) for the first time. The growth window~~ and pre-PCI~~growth window~~ (two weeks leading up to the PCI~~growth window~~) are shown in dark~~blue~~ and light grey~~orange~~ shading, respectively.

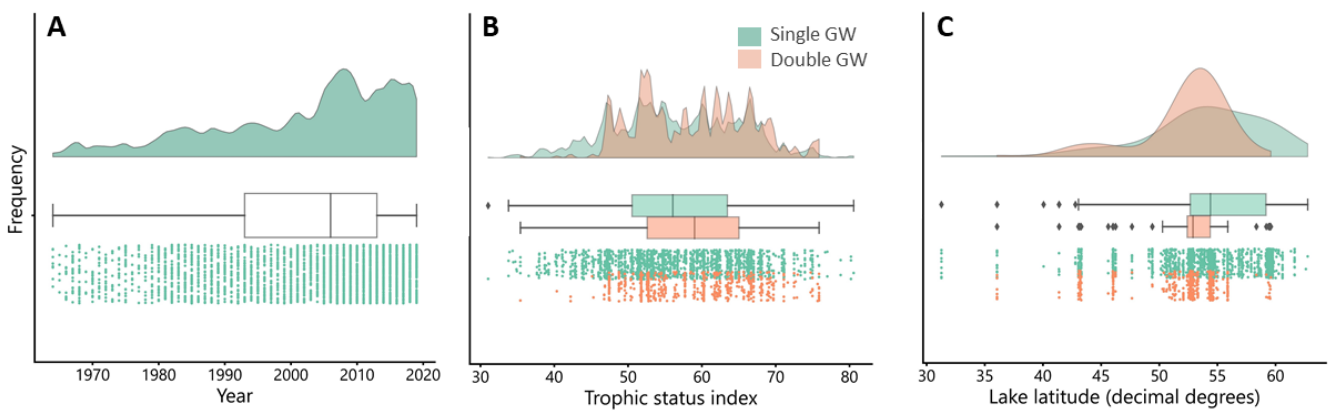

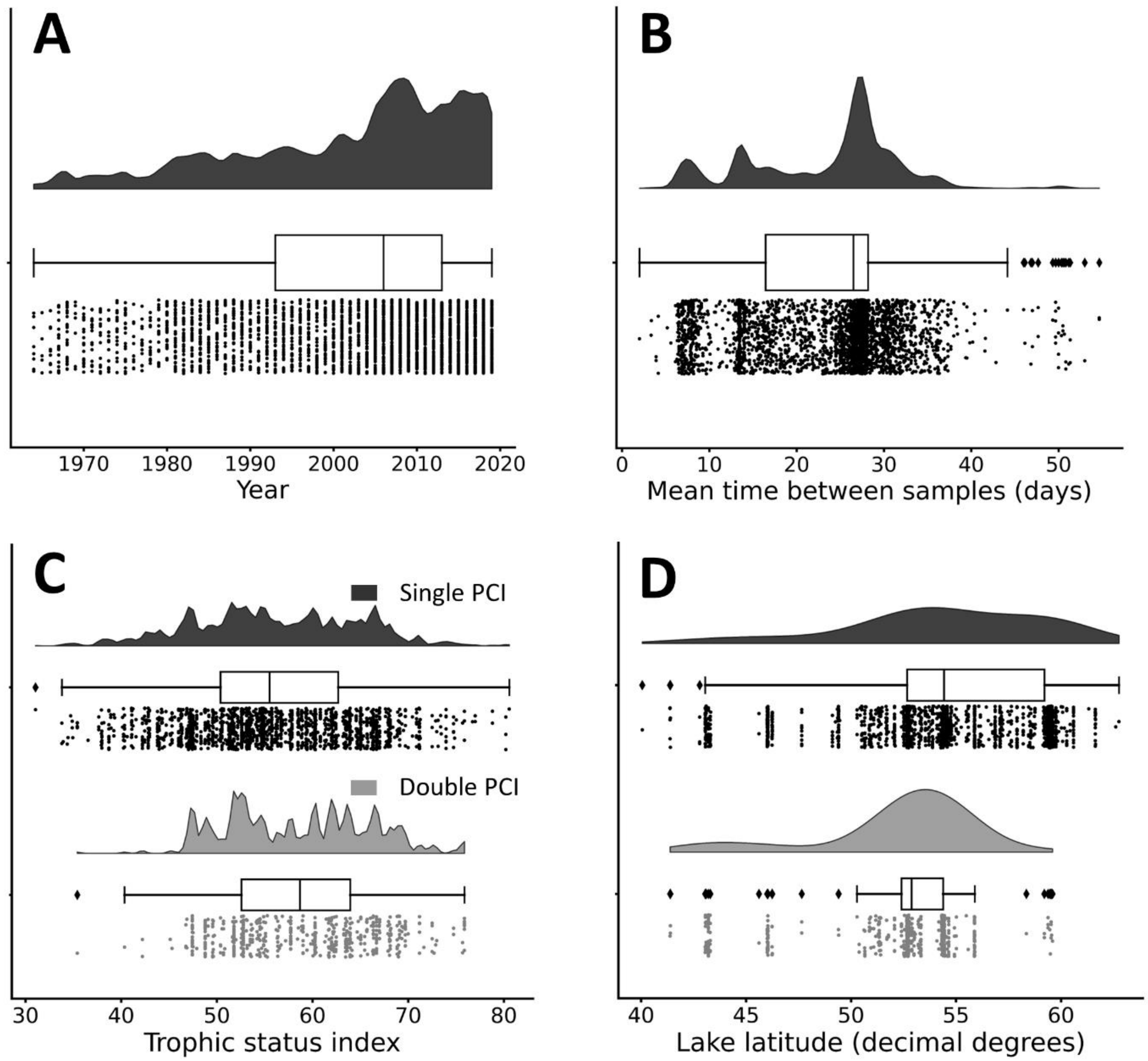

Figure 4. Distributions of (a) year of occurrence, (b) mean time between samples, (c) lake trophic status index, and (d~~c~~) lake latitude for each PCI~~growth window~~ in the dataset. Data are grouped by “double PCI~~GW~~” or “single PCI~~GW~~” year. The data is skewed toward more recent years and higher latitudes. Lakes in the oligotrophic category (TSI < 40) have a higher~~the highest~~ proportion of single PCIs. These “raincloud plots” show the same data visualized in 3 different ways for each group: frequency distribution, boxplot with quartiles (outliers as represented as points), and a jitter plot of data points as different ways to visualize the data (Allen et al., 2021) *(Allen et al., 2021). Note that the amplitude of the frequency distribution is not proportional between categories~~growth windows~~.*

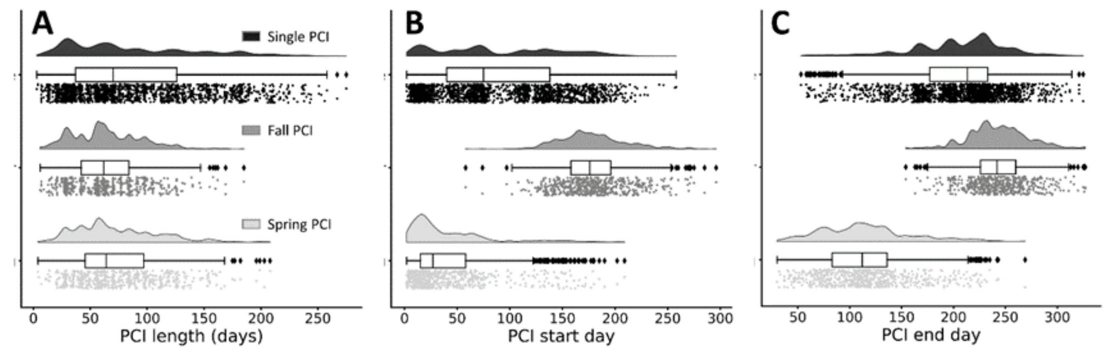

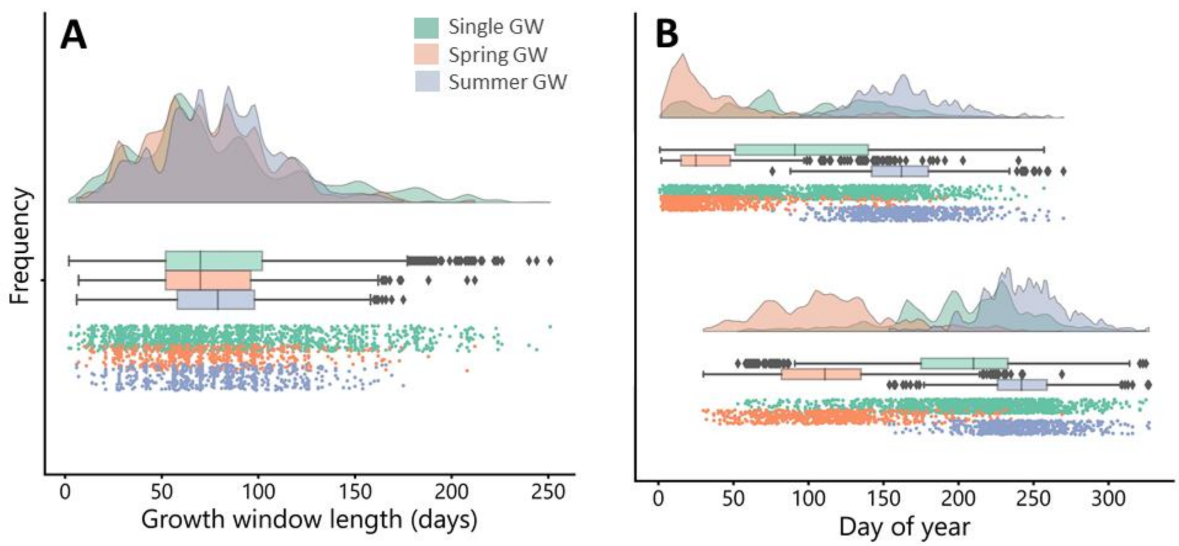

Figure 5: Frequency~~.~~ Distributions of (a) duration, (b) start day (day of year), and (c) end day (day of year),~~b) timing~~ of the PCIs~~growth windows~~, grouped by PCI~~growth window~~ type. Single PCIs~~growth windows~~ have ~~both~~ the longest range in length while fall PCIs tend to be ~~and~~ the shortest. Single PCIs have the largest range of start and end days while the spring and fall PCIs tend to start and end within a smaller window. These raincloud plots show the same data visualized in 3 different ways for each group: frequency~~most even~~ distribution, boxplot with quartiles (outliers represented as points), and a jitter plot of data points.

~~*of start and end dates.*~~

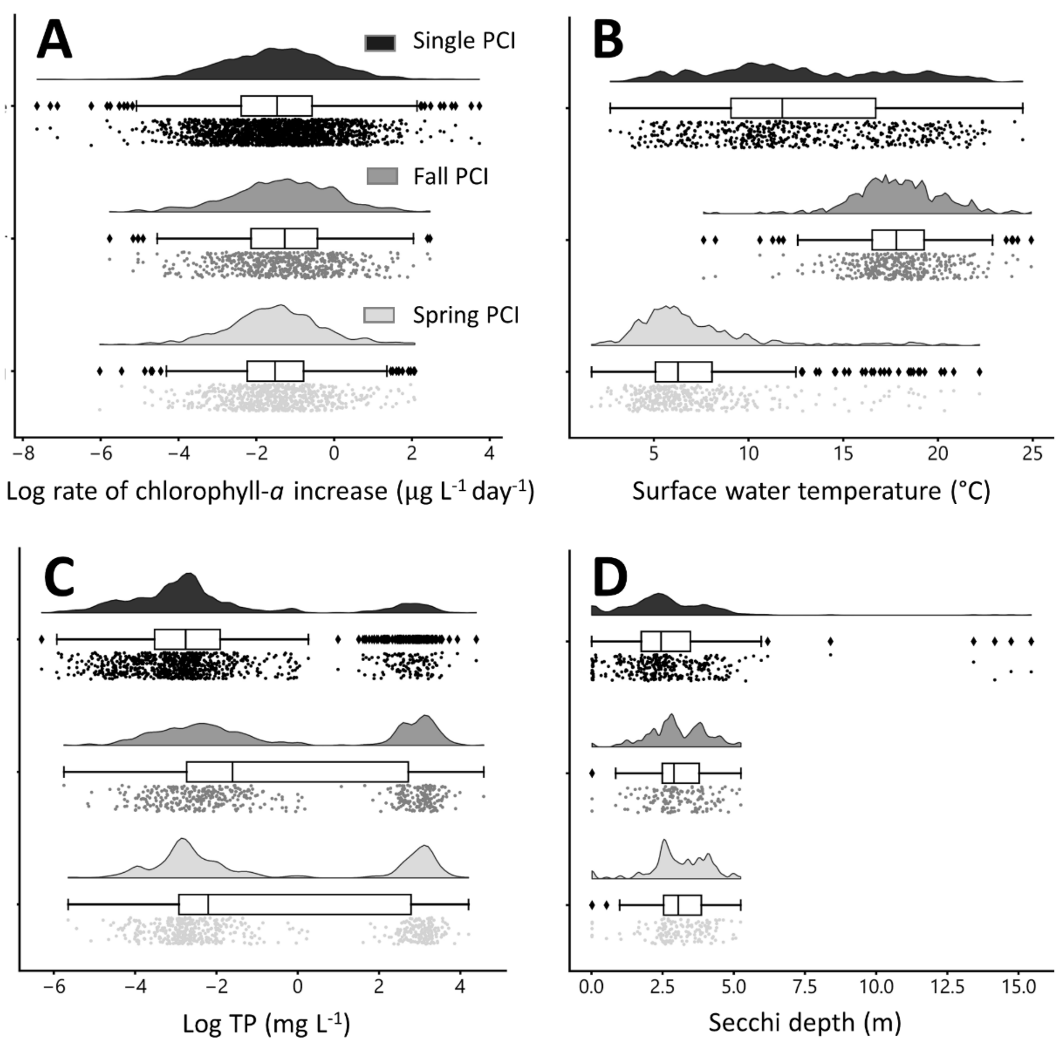
A
Single PCI
Fall PCI
Spring PCI
−8
−6
−4
−2
0
2
4
Log rate of chlorophyll-a increase (µg L-1 day-1)
B
5
10
15
20
25
Surface water temperature (°C)
C
−6
−4
−2
0
2
4
Log TP (mg L-1)
D
0.0
2.5
5.0
7.5
10.0
12.5
15.0
Secchi depth (m)

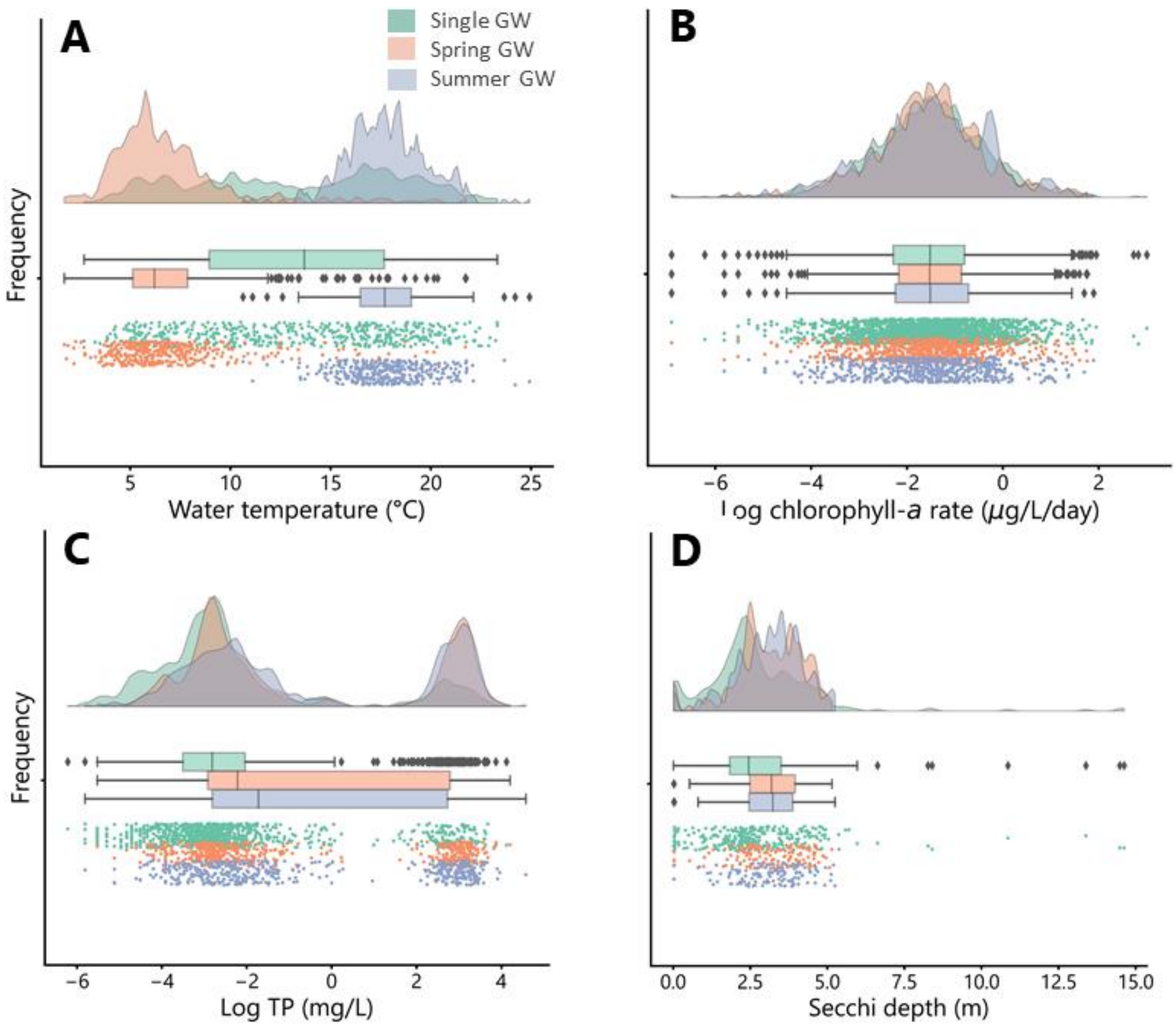

Figure 6. Distributions of selected water quality variables during PCIs~~the growth window period~~: (a) log rate of chlorophyll-a increase~~rate~~, (b) mean surface water temperature, (c) log mean total phosphorus (TP), and (d) mean Secchi depth. The mean rate of chlorophyll-a increase is lowest in the single PCI category and highest in the fall PCIs. For the single PCIs, temperature is evenly distributed across the annual range as they occur throughout the ice-free season. Total phosphorus concentrations are lowest during the spring PCIs, which likely reflects a greater control of P limitation on algal growth during spring compared to summer and fall. Each PCI category has a similar range in Secchi depth, between 0 and 5 m. Raincloud plots show the frequency distribution, boxplot with quartiles (outliers as represented as points), and a jitter plot of data points for each group.

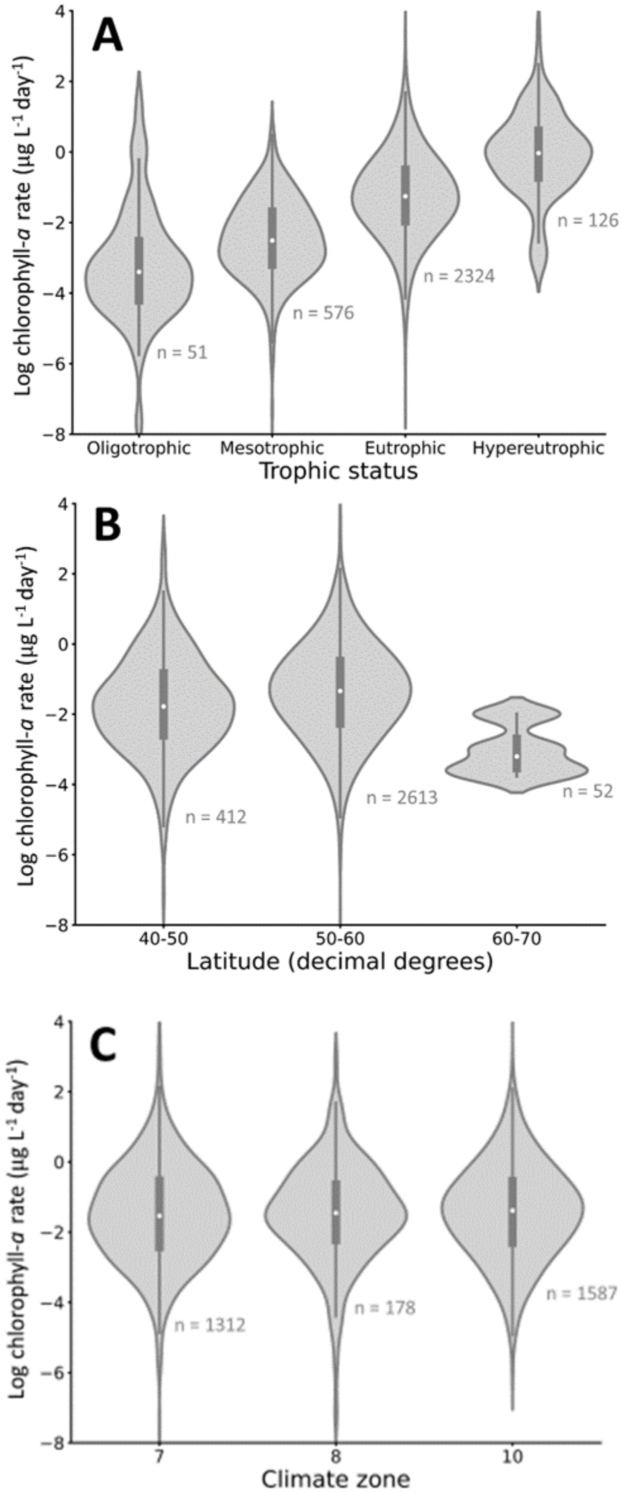
A
B
C
Log chlorophyll-a rate (µg L-1 day-1)
4
2
0
−2
−4
−6
−8
n = 51
n = 576
n = 2324
n = 126
Oligotrophic
Mesotrophic
Eutrophic
Hypereutrophic
Trophic status
n = 412
n = 2613
n = 52
40-50
50-60
60-70
Latitude (decimal degrees)
n = 1312
n = 178
n = 1587
7
8
10
Climate zone

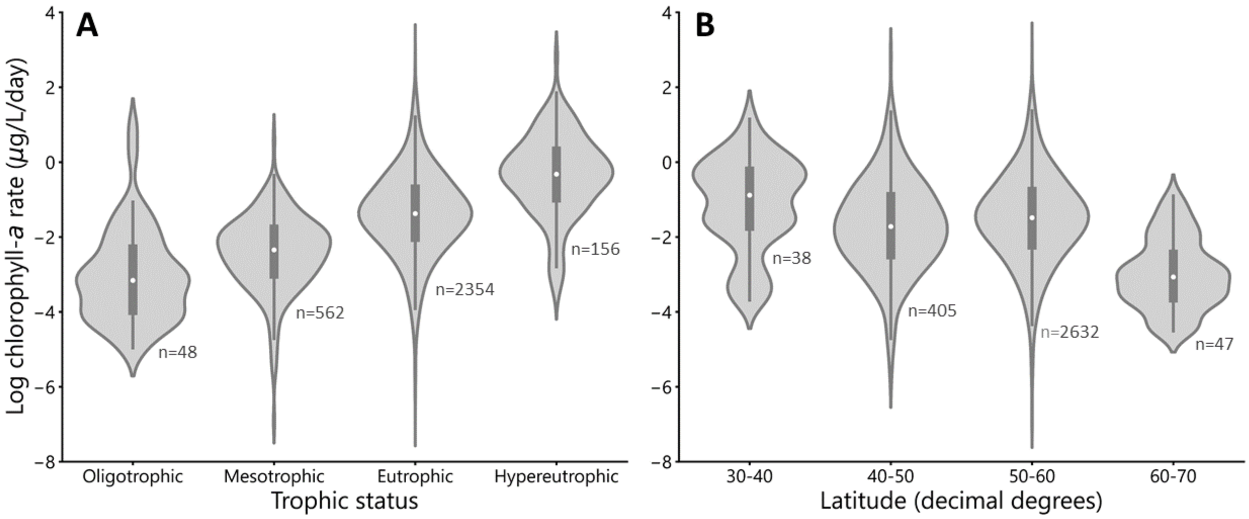

Figure 7. Rate of Chlorophyll-a *increase (RCI)~~growth rate~~ trends in the dataset,~~:~~ grouped by (a) trophic status,~~ and~~ (b) latitude, and (c) climate zone.~~.~~ Lakes of a higher trophic status have a higher mean RCI while ~~chlorophyll-a growth rates and~~ lakes at higher latitudes have lower RCI (with considerable overlap between all categories). Grouping by climate zone shows minimal effect on RCI.~~chlorophyll-a growth rate during the growth windows.~~ The number of lakes represented by each violin is shown in grey text on the panels. Climate zones are as follows: 7 = cold and mesic; 8 = cool, temperate, and dry; 10 = warm, temperate, and mesic. White circles indicate the mean value for each violin.*

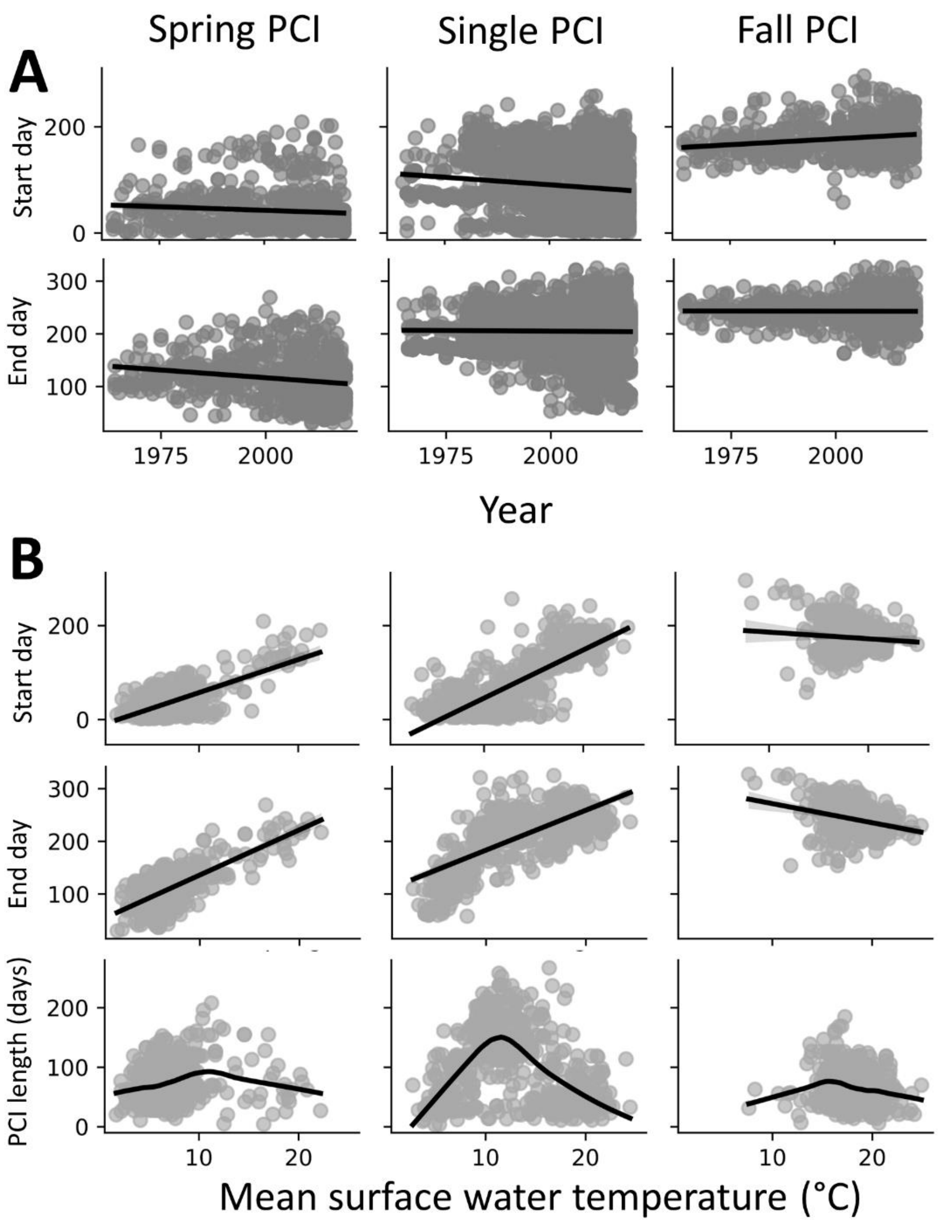
Spring PCI
Single PCI
Fall PCI
A
Start day
End day
Year
B
Start day
End day
PCI length (days)
Mean surface water temperature (°C)

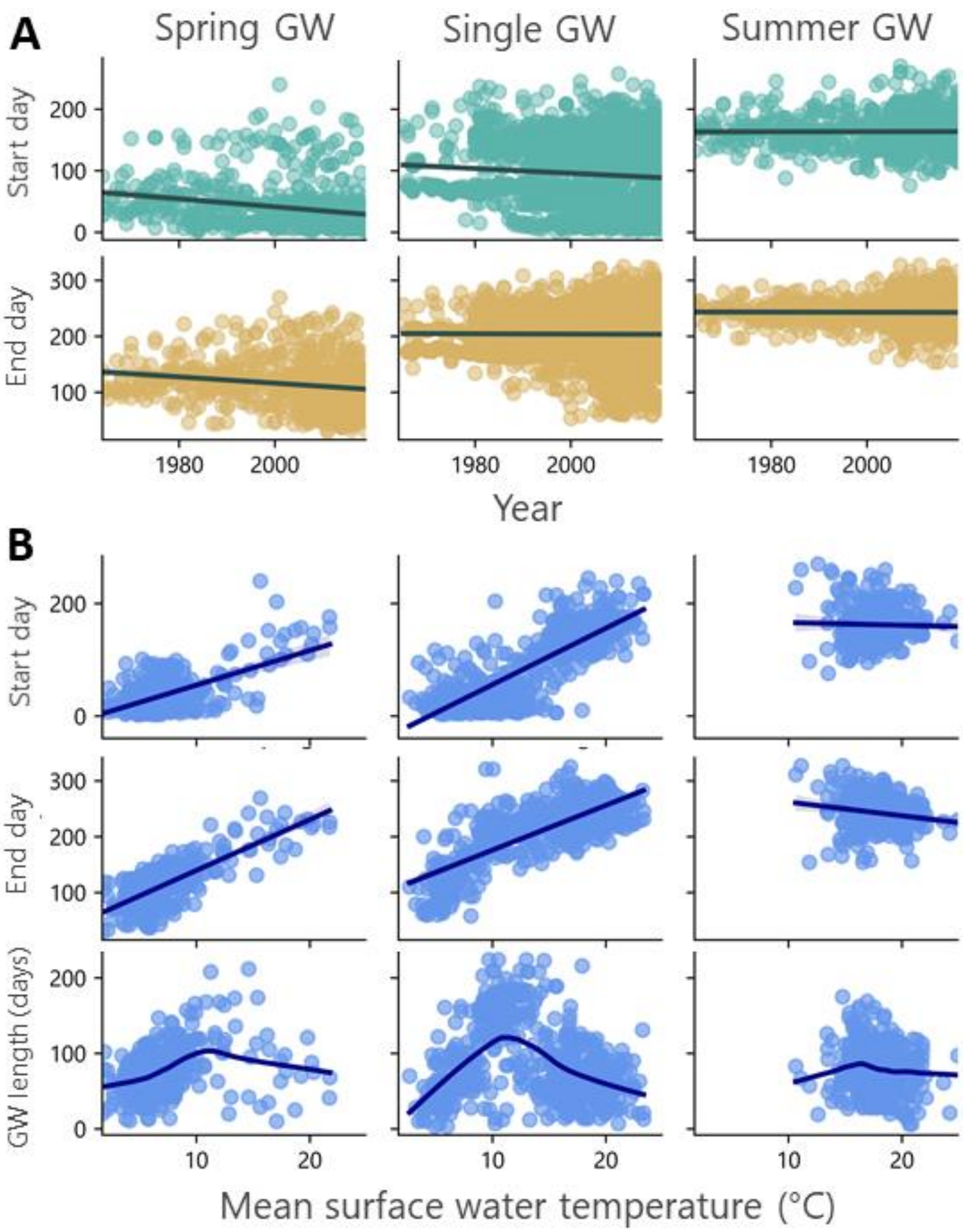

Figure 8. (a) ~~time series of the~~ start and end days~~dates~~ for the spring, fall~~summer~~, and single PCIs~~growth windows~~ for all the lakes in the dataset; spring and single PCI~~all growth window~~ categories trend toward earlier start and end days, while fall PCI start days are occurring earlier~~dates, especially~~ in the year~~spring~~. (b) Start and end days~~dates~~ of the PCIs~~growth windows~~ as a function of temperature (top two rows in panel B, linear regression trendline~~line~~ in black~~dark blue~~) suggest a positive relationship between PCI~~growth window~~ timing and surface water temperature in the spring and a negative relationship in the fall. Longer PCIs~~summer. Growth window length (dark blue trendline shows locally weighted scatterplot smoothing) shows that longer growth windows~~ occur at moderate surface water temperatures which are observed less often during the fall PCIs (trendline fitting data in the bottom row is locally weighted scatterplot smoothing). ~~that aren't seen in the summer months.~~

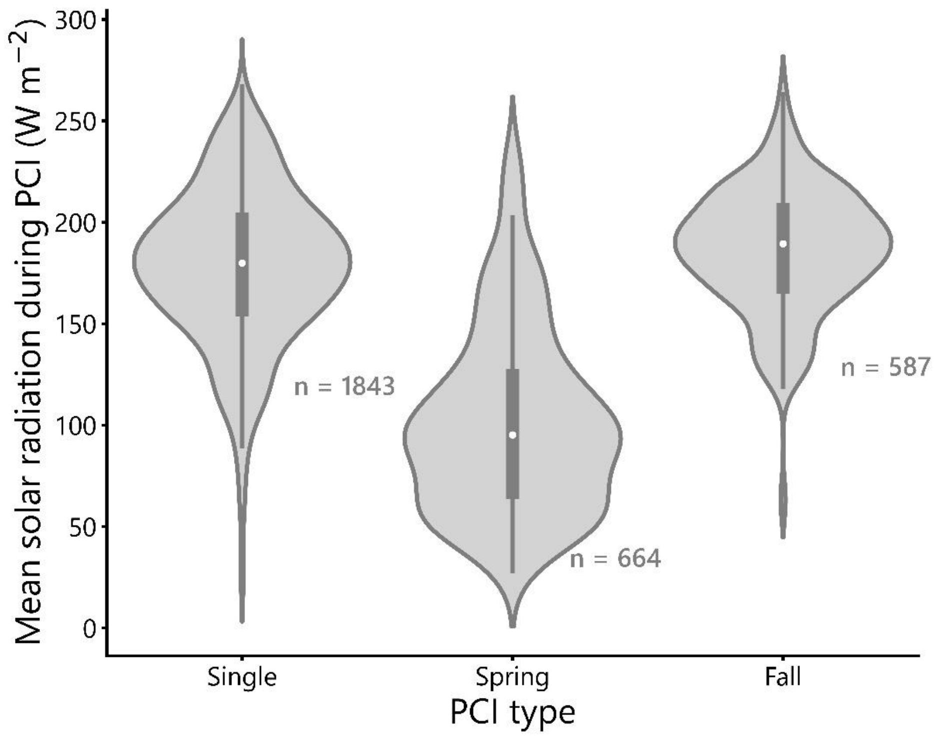

Figure 9: Mean PCI surface solar radiation (SSR) grouped by PCI type (single, spring, or fall). White circles show the mean value for each violin. The mean SSR during spring PCIs is lower than that of single and fall PCIs, which have similar distributions.

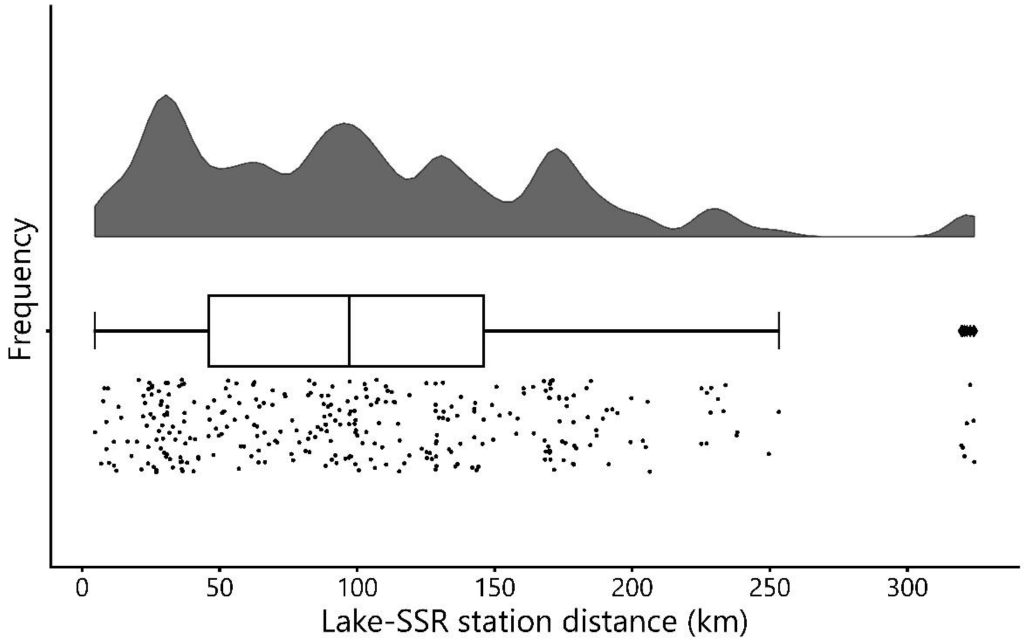

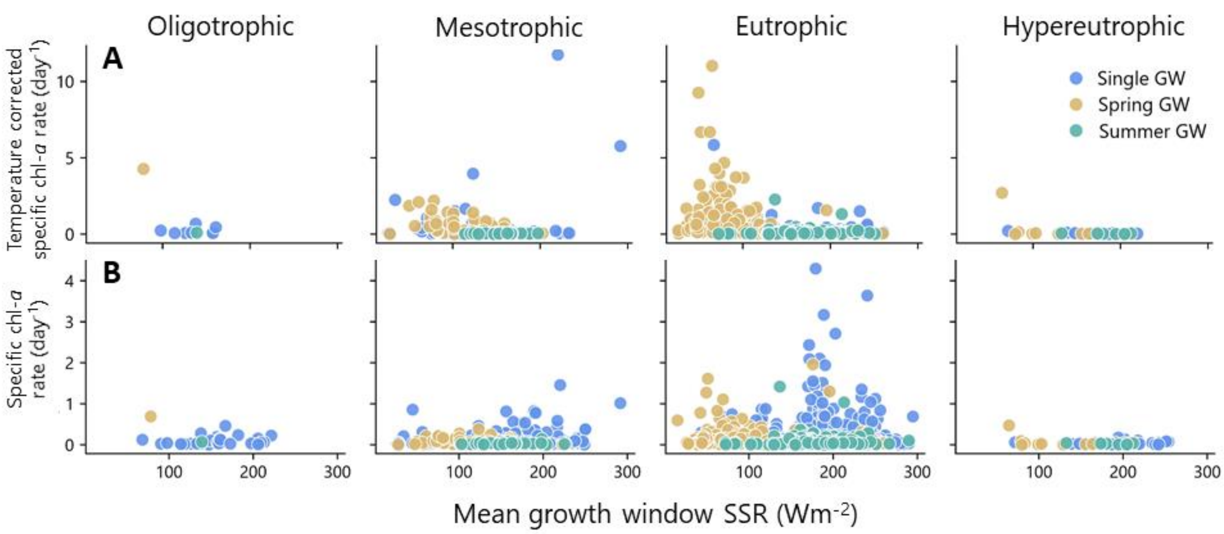

Figure 10: Frequency distribution of distances between the lake sampling points and the nearest surface solar radiation (SSR) sampling stations, in decimal degrees. Most lake-SSR distances are within 200 kilometres of each other. Cloud cover, atmospheric aerosols, and their interactions are a major control on incident SSR at a given surface location, therefore, the SSR values may become less representative of the paired lake with increasing distances. The middle line in the boxplot shows the median value.~~Figure 9. Comparison of trends in the relationship between mean growth window SSR with (a) temperature corrected chlorophyll-a rate and (b) specific chlorophyll-a rate without temperature correction. Data are grouped by trophic status, and hue indicates growth window type. Lakes of a higher trophic status show an increased sensitivity to solar radiation, especially during the spring (panel A) while summer growth windows do not show sensitivity to solar radiation or water temperature, suggesting top-down control from zooplankton grazing. Low chlorophyll growth rates at SSR near or greater than 200 Wm-2 indicate a photoacclimation response in the algae.~~